Fabrication and characterization of biomimetic dry adhesives supported by foam backing material

by

Kelvin Chia Wei Liew

A thesis

presented to the University of Waterloo

in fulfilment of the

thesis requirement for the degree of

Master of Applied Science

in

Chemical Engineering (Nanotechnology)

Waterloo, Ontario, Canada, 2017

Author's Declaration

This thesis consists of material all of which I authored or co-authored: see Statement of Contributions included in the thesis. This is a true copy of the thesis, including any required final revisions, as accepted by my examiners.

I understand that my thesis may be made electronically available to the public.

Statement of Contributions

I would like to state Hamed Shahsavan's theoretical contributions in our co-authored work: "Functionally graded dry adhesives based on film-terminated silicone foam" doi: 10.1016/j.ijadhadh.2017.02.009 published by the International Journal of Adhesion and Adhesives on February 4th 2017, an edited version of which can be found in Chapter 2 "Effect of Foam Backing Material Thickness on Adhesive Properties at Low Preloads" reproduced with copyright permission and the unpublished manuscript presented in Chapter 3 "Multilayer Functionally Graded Material for Dry Adhesive Applications: Scaling from Micro to Macro Terminal Structures".

I would like to state Ephraim (Joshua) Trinidad's 3D design contributions for the millimetre sized mould used in Chapter 3 "Multilayer Functionally Graded Material for Dry Adhesive Applications: Scaling from Micro to Macro Terminal Structures".

All other experimental design, computer programming for data collection, analysis, and writing, are my own or are reused under copyright permission and license, please see Letter(s) of Copyright Permission.

Abstract

Using sacrificial templates to create 3D structures is commonly employed in various fields such as tissue engineering and water remediation to create complex and high surface area scaffolds. Herein, several sacrificial templating techniques are tried, tested, and evaluated and several methods for creating 3D porous material are discussed, including: solvent casting particulate leaching (SCPL) and simple sugar and salt leaching. The porous material is then integrated with polymer soft lithography patterning to create a single functionally graded adhesive (FGA) material to use in dry adhesive applications. The use of a soft foam backing layer helps to improve the compliance and flexibility of the adhesive pad, thus enhancing peel tolerance, buckling, and deflection and vibration resistance.

A dry FGA based on film-terminated silicone foam is developed utilizing the polymer foam's capacity to absorb large amounts of energy and so deliver high adhesion and peel resistance. The fabrication technique is based on simple sugar cube templating of common elastomers, followed by film termination of the polymer cubes using the same material. Dependencies of the pull-off adhesive force and energy release rate on preload and foam thickness are systematically investigated through a series of axisymmetric indentation/de-bonding tests. The contribution of the foam backing layer to the overall compliance and adhesion is analysed and discussed. The developed elastic film-terminated structure strongly enhances the pull-off force and work of adhesion, and can be employed in the transport of delicate objects, as demonstrated in the pick and place of a silicon wafer. Furthermore, the proposed foam-based FGAs can be readily detached from the adherent surface by applying shear deformation between the pad and the surface. This research clarifies the role of mechanical graded properties in adhesion and can have technical implications in the development of a simple but effective dry adhesive material for mounting and transporting objects using automated robotic devices.

The film terminated dry adhesive pads were further developed to investigate the feasibility of using a foam backing material as a universal platform to improve the adhesive properties of other terminal surface morphologies. Integrating other fast prototyping technologies as an alternative to lithographic templating

techniques, scaled acrylonitrile butadiene styrene (ABS) 3D printed mushroom capped terminal structures are determined to be comparable to polyacrylate microstructure templated moulds. The effect of the foam is systematically evaluated using a similar axisymmetric indentation/de-bonding test with a probe of a large radius of curvature. Contact splitting through the control of terminal structures in both micro and millimetre scales shows improved contact properties with the addition of foam backing material. The mushroom capped adhesive pads are employed to demonstrate shear peel tolerance and cold temperature surface tolerance demonstrations.

Lastly, various sugar and salt templating techniques are explored and optimized for consistency and repeatability to select the material most suitable for current research. Statistical analysis is used in the selection process. A linearly approximated model to determine the pull-off force from foam porosity and stiffness parameters are reported as sample candidates. Model estimates find that the density of sugar granules and the applied preload force are the mostly significant contributors to increasing pull-off force.

Acknowledgments

Writing assistance: Mary McPherson, a Writing and Multimodal Communication Specialist at University of Waterloo's Writing and Communication Centre.

Research group members: Li Chen, Aleksander Cholewinski, Zihe Pan, Hamed Shahsavan, Josh Trinidad, Jeremy Vandenberg, and Kuo Yang for their advice, laboratory assistance, valuable discussions, and friendship.

Supervisor: Dr. Boxin Zhao for access to his laboratory and group's expertise and providing the numerous opportunities to help me develop into an academic researcher.

Funding: University of Waterloo and National Sciences and Engineering Research Council of Canada for scholarships and grants.

Dedication

I dedicate this thesis to my family:

To my mother and father, for meeting and giving birth to me, for moving to Canada and investing in my education and quality of life, for their unending love and support, and for teaching and instilling curiosity in my nature.

To my sister for her honest opinion and inspirational dreams.

To my Canadian aunt and uncle for housing and starting us out in our new life in Canada long ago.

To my grandparents for their care during my childhood and financial support for my education.

I dedicate this thesis also to my teachers:

To my university mentors Dr. Nasser Mohieddin Abukhdeir and Dr. Chris Backhouse for their personal interest in nurturing my academic career.

To my lab instructors Jenn Coggan, John Saad, and Howard Siu for their expertise, friendship, and career/life advise.

To my high school teachers, Jacqueline Glendenning, Wendy Grandin, Joe Hall, Nick Lacoppola, Marios Papagapiou, Elisabeth Pocsai, Espedito Schiafone, Robert Yu, and many others for building my love for math, science, and technology.

To my university friends, Aaminah Ahmad, Tessa Alexanian, Zachary Jacobi, Sabrina Li, and Ryan Neufeld, who provided their friendship, helped diversify my interests, cultivated my personal ethics and philosophy, and rounded out my sharp edges.

Table of Contents

List of Figures

List of Tables

List of Abbreviations

(in order of appearance)

3D	3-dimension
SCPL	solvent casting particulate leaching
FGA	functionally graded adhesives
ABS	acrylonitrile butadiene styrene
SEM	scanning electron microscope
PDMS	polydimethylsiloxane
PU	polyurethane
FGM	functionally graded materials
EPS	expanded polystyrene
SCPL	solvent casting particulate leaching
SMPL	solvent merging particulate leaching
PLGA	poly(lactic-co-glycolic acid)
NP	nanoparticle
DI	deionized water
FDTS	(heptadecafluoro-1,1,2,2-tetrahydrodecyl)trichlorosilane OR trichloro(3,3,4,4,5,5,6,6,7,7,8,8,9,9,10,10,10-heptadecafluorodecyl)silane
UMT	universal mechanical tester
IFD	indentation force deflection
ABS	acrylonitrile butadiene styrene

List of Symbols

(in order of appearance)

μ	porosity
φ_0	relative density
ρ	density of the foam
ρ_s	density of the constituent material
t	thickness of the terminal layer
S	surface stiffness, i.e. the slope of unloading portion of force-displacement curve
C or C'	surface compliance or effective compliance
F or F_z	pull-off force in the z-direction (tensile)
δ	displacement
F_{max}	pull-off force
W_{adh}	work of adhesion
a/h	confinement parameter
f_c	geometrical correction factor
C_B	Boussinesq compliance
f_c	geometrical correction factor
E or E^*	Young's modulus or reduced Young's modulus
ν	Poisson's ratio
A_0	geometric constant of proportionality
E^s	tangent modulus of a parent solid
U_{hys}	hysteresis of an adhesive
∅	diameter

"God made the bulk; surfaces were invented by the devil." - Wolfgang Ernst Pauli in Growth, Dissolution, and Pattern Formation in Geosystems (1999) by Bjørn Jamtveit and Paul Meakin, p. 291

Chapter 1. Introduction and Literature Review

The objective of the thesis is to use a soft backing material to improve the adhesive properties of dry adhesives. This is achieved in *three* steps corresponding to each research chapter of the thesis. The thesis is organized as follows: Chapter 1 "Introduction and Literature Review" discussing leading research and theories of contemporary structures and concepts currently employed in dry adhesives as well as some background literature on polymer foam fabrication, Chapter 2 "Effect of Foam Backing Material Thickness on Adhesive Properties at Low Preloads" – my published work studying the behaviour of preload and foam backing material thickness on pull-off force, Chapter 3 "Multilayer Functionally Graded Material for Dry Adhesive Applications: Scaling from Micro to Macro Terminal Structures" – an unpublished manuscript exploring the universal platform of foam backing materials using different terminal structures at micro and macro scales, and Chapter 4 "Compression Study on Foam Porosity" reports the effects of foam porosity and stiffness on pull-off force, leading to the optimization of material fabrication of the previous two chapters.

The rationale of the research chapters are as follows: Chapter 2 describes the systematic study of the foam thickness and its improvement in adhesion strength compared to a simple polymer block. This work is expanded upon in Chapter 3 where mushroom capped terminal structures were explored at both micron and millimetre scales to determine if foam backing improves the adhesive properties of different sized and geometries of terminal structures, thus making it a general design parameter rather than a terminal structure specific one. Lastly, in Chapter 4, *four* sugar cubes with different porosities and stiffness values were tested and statistically analysed to select the best foam porosity/stiffness that will result in optimal adhesion properties.

This thesis includes work in *two* main fields: dry adhesives and polymer foam templating. Within dry adhesives, the concept of compliance: the ability of the adhesive to maximize contact with the adherent surface, is the linking agent between these fields. Dry adhesives are a developed area of biomimetic polymer materials science focused on using various polymeric materials and patterning methods to design complex

surface features reminiscent of the Gecko toe pads for applications in material bonding. The adhesive properties are generated from van der Waals interactions rather than chemical intrusion and bonding. This is achieved through material templating techniques such as soft lithography which allows pattern transfer from silicon materials to polymeric elastomers. The field of dry adhesives has defined various terminal geometries, feature aspect ratios, and contact mechanic theories to assist in the design and understanding of adhesive materials which has led to directional fibrillar materials able to hold kilograms of load.

However, there has been little research done on modifying the material configuration of the backing substrate of dry adhesives. Herein, the theory of compliance plays a large role. Compliance is how easily the adhesive can match the surface to which it is bound. Having better compliance means allowing more contact area between the surface and the adhesive. To achieve this, flexible fibrillar structures are currently being investigated due to improve contact on rough surfaces. These fibrillar structures with delicate terminal features only span lengths of nano to micrometres, leaving the millimetre region largely unexplored. After all, the Gecko, nature's analogue, has millimetres of "soft" fleshy material backing its famed fingertips.

Thus, the field of polymer foams can simulate the soft equivalent of flesh. Currently, popular polymer templating methods uses a sacrificial water-soluble particulate to create a 3D mould for the prepolymer. Once the prepolymer is cured, the particulate is removed by water dissolution, leaving a bi-continuous gyroid polymer foam, the other phase being air. Modifying this templating method, a soft foam backing material with attached fibrillar structures is fabricated and its adhesive properties measured.

1.1. The Gecko

The gecko lizard is one of nature's solution to a sticky problem. Recent research been completed looking at their foot pads to determine how their climbing ability maybe exploitable to create synthetic dry adhesives. The gecko toe pads, as seen in Figure 1, consists of a hierarchal system of flexible hairs with a directional attachment mechanism. Autumn et al.'s investigation into a single seta's adhesion performance in parallel and perpendicular release direction to a surface seen in Figure 2, estimates that a $1cm^2$ adhesive pad is able to produce $10N$ of adhesive force resulting in a lower limit estimate of $20\mu N$ per seta at approximately 5000 setae per square millimetre [1]. Autumn et al. has also shown in various movie clips

and slow motion video analysis, that the gecko accomplishes this directional control by attaching and detaching its toe pads with the curling of its toes into and away from the surface [2].

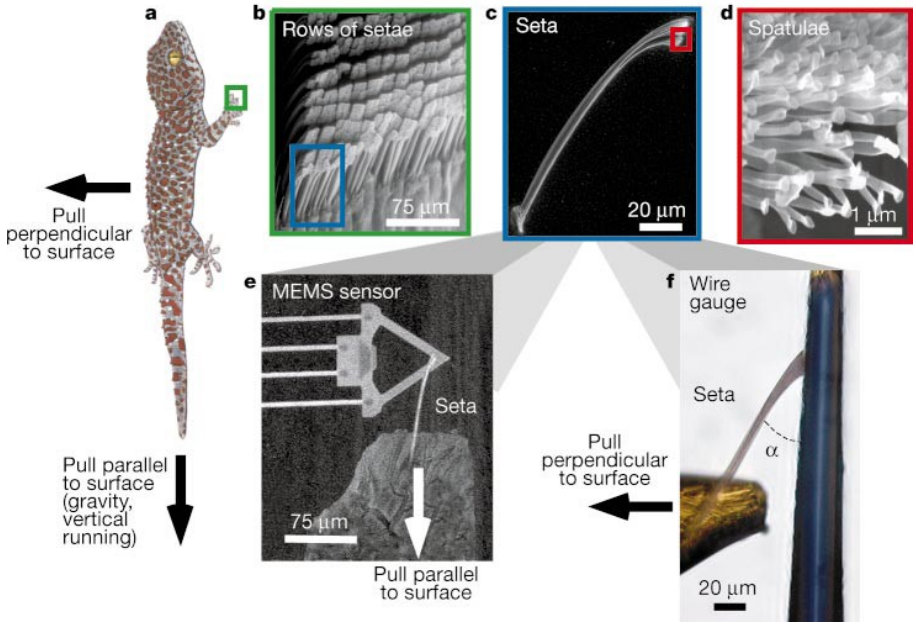

Figure 1: (a) A Tokay gecko (Gekko gecko); SEM of setae from toe pad of animal: from (b) rows of setae to (c) single seta and finally the (d) fine terminal branches of the spatulae; (e) a single seta attached to a MEMS cantilever to conduct parallel and perpendicular attachment-detachment tests on (f) an aluminium bonding wire. Reproduced with permissions from Nature Publishing Group [1].

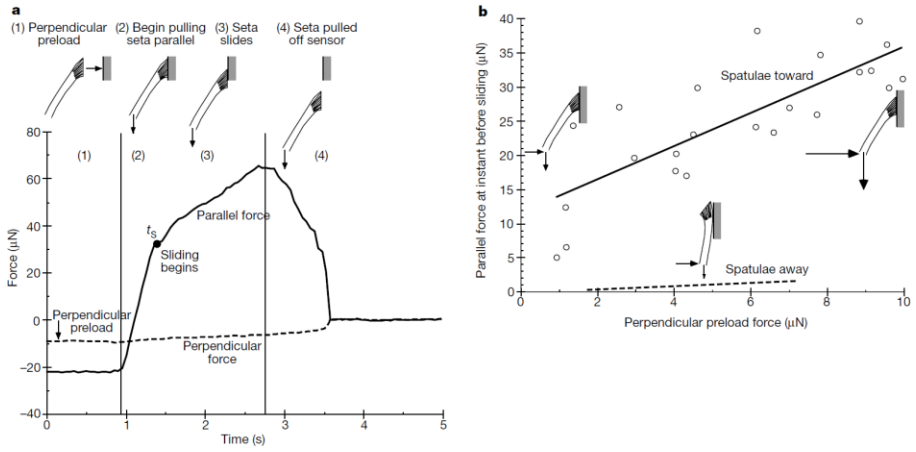

Figure 2: (a) Perpendicular preload and parallel sliding pull-off test showing (b) preload dependence of single seta from gecko toe pad. Reproduced with permissions from Nature Publishing Group [1].

1.2. Dry Adhesives

Dry adhesives are a class of adhesives where adhesion is reliant only on non-covalent bonding forces; generally, physical interactions like van der Waals force [3], [4], hydrogen bonding, charge interactions, suction, capillary effect, etc. whose individual force is small, but at critical mass can have an overall effect. Most adhesives familiar to the public are chemical adhesives: wood glue, epoxy, clear tape, post-it notes, etc. These adhesives use chemical bonding force between the surface and a semi-flowable "wet" layer of chemicals. However, they are usually single use or deteriorate with each application and leaves surface contamination/residue. In contrast, dry adhesives, can be regenerated by cleaning with a light solvent or by self-cleaning mechanisms. The drawbacks of dry adhesives are its high cost, complexity, lower overall adhesion performance, and lacking rough surface adhesion, thus limiting their use to light and relatively smooth surface applications.

1.2.1. Compliance

Compliance can be defined as the change in displacement over force at maximum contact area [5]. It is linked with the ease of which the adhesive can contact the adherent surface. Chemical adhesives maximize the requirement of intimate contact by using its wet adhesive layer to intrude into the surface, filling in gaps and increasing surface contact area (before curing for permanent adhesives). Dry adhesives need to use more flexible and small terminal end structures to reach deep into the microscopic and often nanoscale valleys and peaks. Although there has been a plethora of work on the terminal surface of dry adhesives, these complex fibrillar structures are complaint mostly only at short distances, while the backing material's larger range has garnered less attention. Within this work, compliance will be generalized as the ability of the material to reach and increase its contact with the surface.

1.2.2. Terminal Structures

The simplest terminal structure for dry adhesives is the surface of a block of polymer material. Due to differences between the surface and bulk, the bulk will only experience cohesive forces, while the surface will experience a combination of cohesive and interactive (adhesive) forces with whatever medium it might be in contact with, e.g. air, water, etc. One higher level of complexity is the pillar or hole structure, where

there is a continuous or confined air gap between surface features at uniform and regular spacings. Complexity can drastically reduce the potential surface contact area depending on the packing and spacing of the patterned features, but can also improve energy dissipation. The aspect ratio of the features can also play a role; if the pillars are too long they will collapse via *three* mechanisms ground collapse, lateral collapse, and capillary collapse as seen in Figure 3 [6].

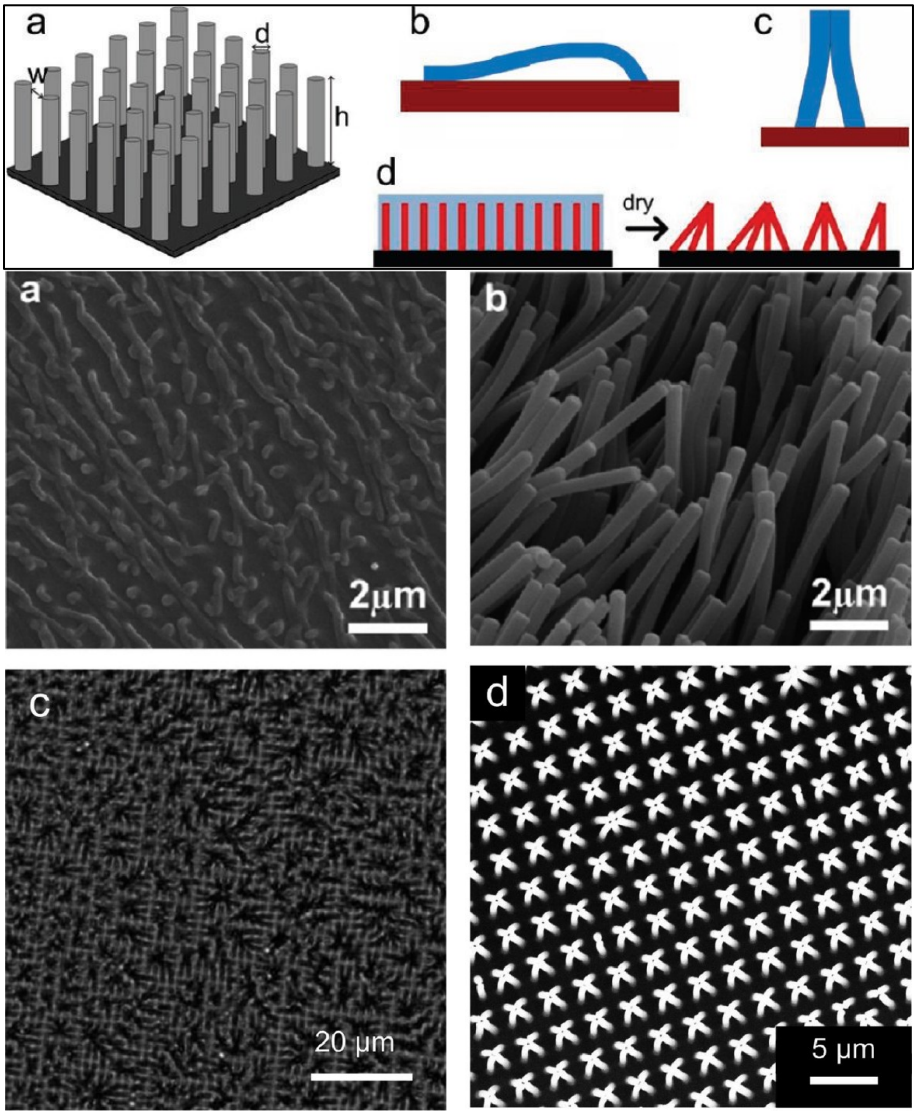

Figure 3: (top) Mechanical failure modes of (a) high aspect ratio pillar arrays: (b) ground, (c) lateral, and (d) capillary collapse; (bottom) SEM images of collapsed (a) PDMS, (b) PU, and (c, d) poly(ethylene glycol) dimethacrylate hydrogel pillars. Reproduced with permissions from American Chemical Society [6].

Many other structures can be created by adding onto and/or modifying the pillar structure: straight, tilted, curved, spiral supports, etc. These pillars generally act as a spring between the bulk polymer block and the surface, fulfilling energy damping and dissipation functions. Additionally, structures can be placed atop these fibrillar supports: film terminated [7], mushroom [8], spatula [9], and even hierarchical levels [10] of any combination as seen in Figure 4, Figure 5, Figure 6, and Figure 7. Their development is widely inspired by the multilevel hierarchical nature of biological analogues such as the gecko lizard.

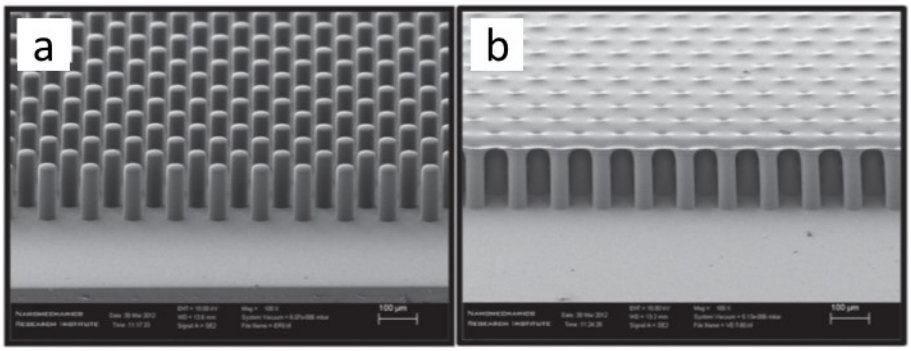

Figure 4: SEM of (a) 50µm diameter, 150µm high micropillars, and (b) topped with an 8µm thick film; scale bar at 100µm. Reproduced with permissions from Royal Society of Chemistry [7].

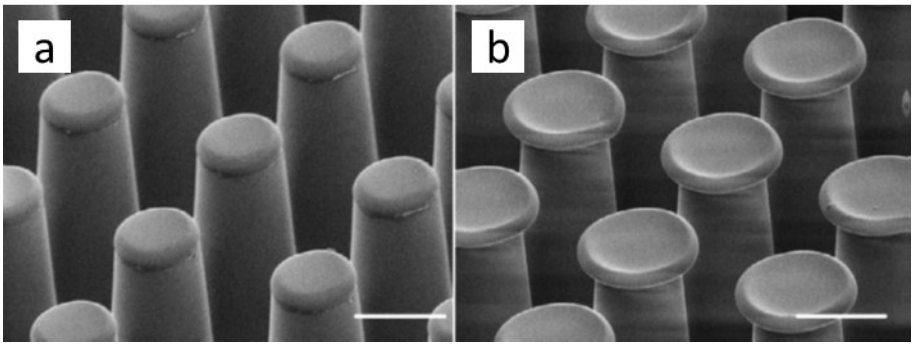

Figure 5: SEM of (a) undecorated pillars; (b) mushroom capped terminal end; scale bar at 10µm. Reproduced with permissions from Institute of Physics Publishing [8].

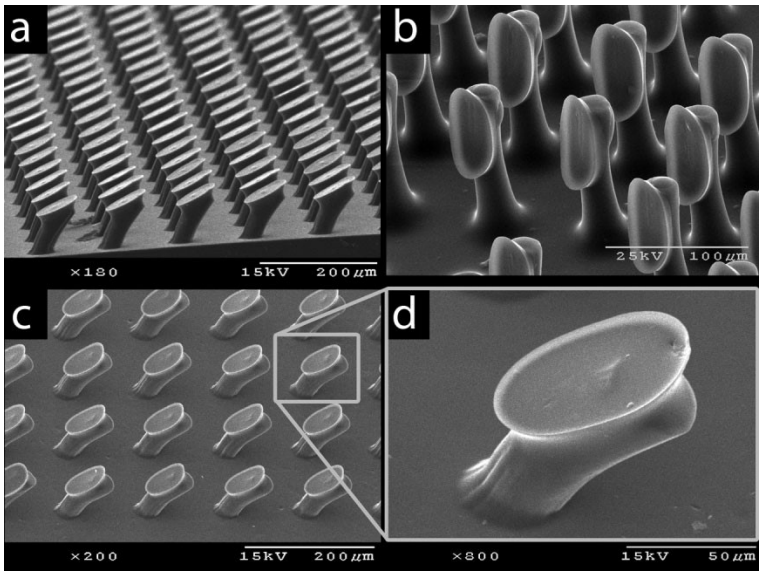

Figure 6: SEM of 35μm diameter angled PU microfiber arrays with angled mushroom caps. Tip orientation at following angles: (a) 34.8°; (b) 90.8°; and (c, d) 23.8°. Reproduced with permissions from John Wiley and Sons [9].

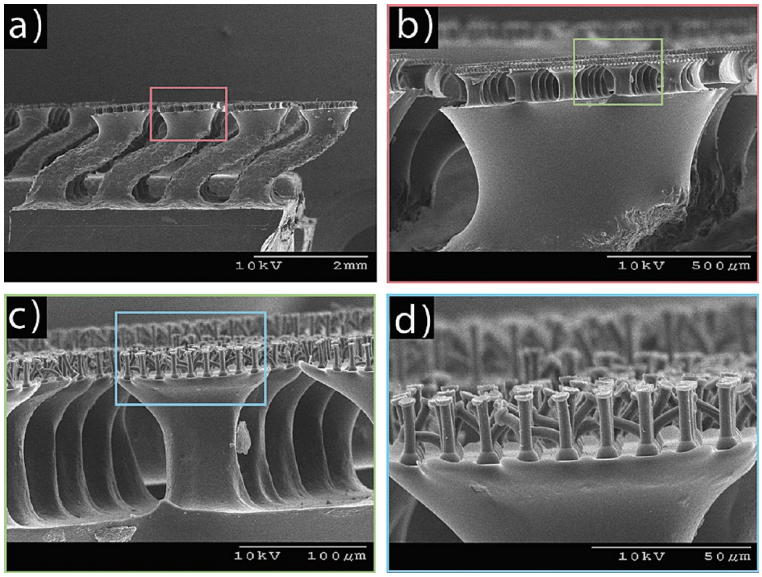

Figure 7: SEM of three-level hierarchical PU fibres: (a) 400μm diameter curved base fibres; (b) zoom-in of base fibre tip with midlevel 50μm diameter fibres; (c) zoom-in of midlevel fibres; (d) zoom-in of terminal third level 3μm diameter, 20μm high fibres with 5μm diameter flat mushroom caps. Reproduced with permissions from American Chemical Society [10].

1.2.3. Contact Geometry and Splitting

The generalization of contact splitting is that the more pieces that the surface is broken up into, the more energy can be dissipated by the adhesive [3], [11]. Having only a film terminated fibrillar structure for example, is not very peel tolerance due to the propagation of a peel front once it has been initiated. The initial pull-off force is high as energy is expended to overcome edge effects of the adhesive film; however, once a front has begun, it is easier to continue peeling due to stresses at the interaction point. In contrast, if the same film terminated fibrillar structure is split into many smaller sections (even if there is less overall contact area), it will perform much better as each structure has its own energy barrier preventing propagating of the peel front throughout the rest of the adhesive pad.

Furthermore, the contact geometry also plays a significant role in the control of adhesive properties, more so than surface chemistry [3]. This has been extensively evaluated by Bartlett et al. creating a general design parameter relating the contact geometry to a resulting force capacity [13], [14]. As mentioned previously, radially symmetrical [8] and asymmetrical [9] terminal structures will restrict which direction peeling will more easily occur. Parallel to tilted pillars, it is easier to peel from one direction than its opposite direction. This behaviour can be observed with spatula terminated ends, as it is not centred on the supporting structure, the shorter side is easier to detach than its longer end.

1.2.4. Functionally Graded Materials

FGAs are another class of materials where there is a gradient in mechanical and/or chemical properties along the thickness of the material, as seen in Figure 8 [5]. In terms of dry adhesives, functionally graded materials (FGM) can be the terminal structures, followed by the supporting structure, and finally the backing substrate. In the presented work, the softness/flexibility of the graded materials with relation to adhesive properties are investigated i.e. different terminal structures resting on pillar supports on foam or block backing substrates.

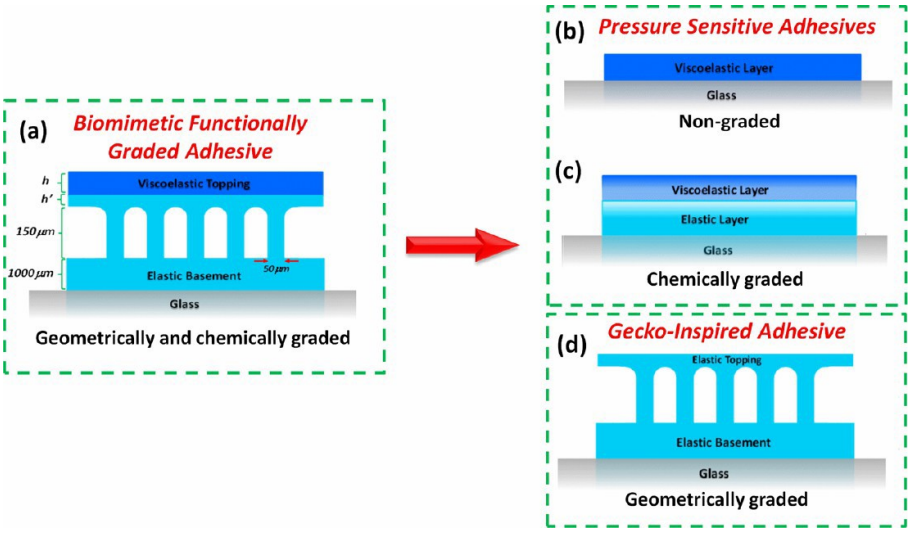

Figure 8: Schematic of (a) bioinspired FGA with viscoelastic chemical and geometrically graded layer atop an elastic substrate on a glass substrate, (b) a simple viscoelastic layer on glass, (c) a viscoelastic layer atop an elastic polymer on glass, and (d) an elastic film terminated biomimetic fibrillar adhesive on glass. Reproduced with permissions from American Chemical Society [5].

1.3. Polymer Foams

Foams are 3D low-density materials that exhibit large voids and cavities of empty regions, resulting in high surface area and being light in weight. They can be extremely flexible and compressible if the component material is elastic and can have closed or open cell structures. Due to its high surface area, it is used in many energy absorption/dissipation applications/devices, such as noise cancellation, thermal dissipation/insulation, packaging, as a filler material, sensors, safety equipment, as well as chemical adsorption, and 3D templating.

There are a few methods of creating dry solid polymer foams: using fast acting/curing polymerization reactions, high temperatures and a pressure differential, or using physical agitation and confinement. Spray foam insulation is an example that uses an isocyanate and polyol resin (PU) that can expand several times its liquid volume, trapping air within its closed cell structure. Commonly used in construction and other lightweight insulation applications, this material cures stiffly and can be sprayed into a mould of a desired geometry [15]. Its soft polyurethane counterpart: memory foam, is made with di-

isocyanates and polyols, once mixed it reacts into a soft open cell structure that is later cured into its final soft state [16]. These foams are used for furniture and packaging.

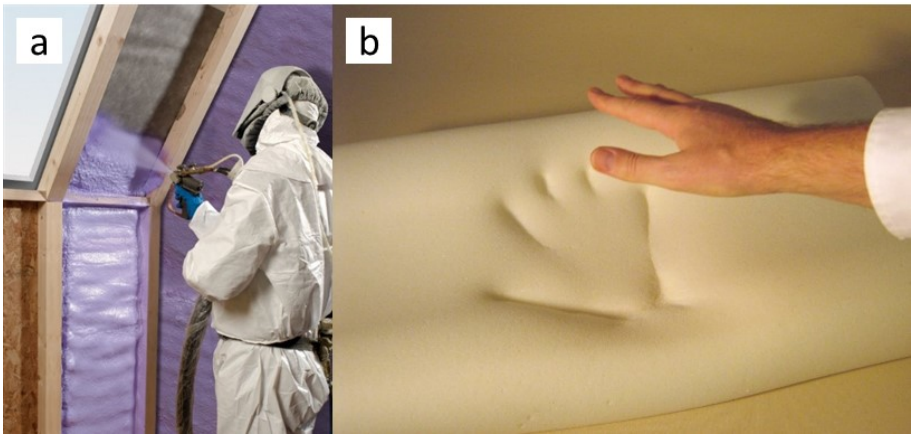

Figure 9: Photograph of (a) spray foam, credits: Cdpweb161 as hosted on Wikipedia, CC BY-SA 3.0 and;(b) memory foam, credits: Johan as hosted on Wikipedia, CC BY-SA 3.0

Another stiff closed cell foam: packing foam, uses expanded polystyrene (EPS) via high temperature liberation of trapped gases from volatile compounds that results in a volume increase of 40-50 times. After confining in a mould, steam is used to fuse the individual pellets together resulting in a 98% porosity material [17].

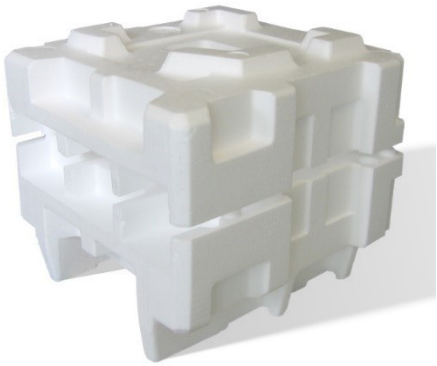

Figure 10: Photograph of EPS packaging foam, credits: Acdx as hosted on Wikipedia, CC BY-SA 3.0

1.3.1. Contemporary Studies on Polymer Foam/Sponge Casting

Solvent Casting/Particulate Leaching

Previous examples of foam production are commercialized industrial processes; in this section, the research methods of making dry foams using a sacrificial template (porogen) will be discussed. Sugar and salt are commonly used in this technique as the granules can be removed via water infiltration and dissolution.

Solvent casting/particulate leaching (SCPL) technique is a process of dispersing polymer in an organic solvent, followed by the incorporation of water soluble particles into the solution before moulding [18]. A polymer-particulate composite is formed after solvent evaporation before porogen leaching. Liao et al. uses salt, which is easily removed by leaching in a water bath, resulting in a porous polymer structure with controllable pore size and porosity. The choice of salt particle size and its weight percent to the polymer solvent mixture determines the void dimensions [18]. SCPL's inherit issue stems from its non-uniformity coating and frequent particulate encapsulation by the polymer, blocking later leaching [18].

Liao et al.'s modification of SCPL, solvent merging particulate leaching (SMPL), uses solvent assisted polymer fusion of a dry mixture of poly(lactic-co-glycolic acid) (PLGA) a biodegradable polymer, and salt granules. The modified SCPL technique directly incorporates the polymer and salt into a mould before being chased by the polymer solvent. The liquid flows through the voids between the solid mixture, fusing the polymer particles. A polymer non-solvent is pulled through to precipitate the polymer, followed by flushing with water to remove the salt. The schematic of the process and the resulting material is shown in Figure 11.

The PLGA scaffolds are created by grinding PLGA grains and sieving it through 250-470μm mesh (No. 40 and 60). The NaCl is also sieved and the dry mix is combined at various weight ratios at room temperature before filling a Teflon container with No. 80 mesh attached to a Büchner flask with 10g of dry mix. The resulting porosity of 85-95% at >100μm pores can be controlled by the PLGA-NaCl weight ratio. Cell and tissue culture applications require high porosity to promote growth, the interconnection of the scaffolding will allow for ingrowth, vascularization, and nutrient transport.

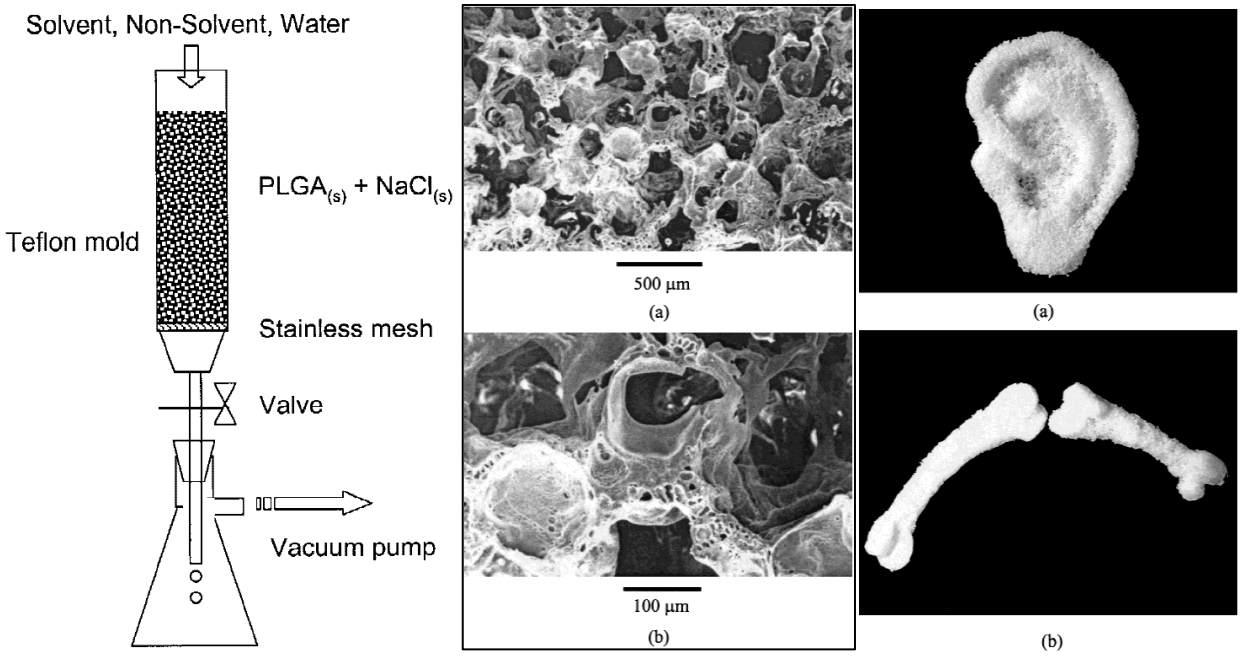

Figure 11: (left) Schematic of the SMPL method with polymer solvent, non-solvent, and water introduced to the dry mix of PLGA and NaCl in succession to produce, (middle) (a-b) SEM images of 3D porous PLGA material, and (right) (a-b) the resulting PLGA 3D scaffolding for tissue and bone growth. Reproduced with permissions from John Wiley and Sons [18].

In-situ Aqueous Casting

Direct mixing of Au nanoparticle (NP) precursor $KAuCl_4$, in PDMS premix is synthesized for aromatic and sulphur water purification and targeted drug release. The choice of polymer and reducing agent is important as they must operate in both roles of NP formation and as a polymer curing agent.

Figure 12 indicates the fabrication route for producing a gel and foam of Au embedded PDMS material. Using a combination of PDMS 10:1 v/v to curing agent, mixed with $0.02M$ aqueous $KAuCl_4$ solution at 200:1 m/v (mg/mL) and stirred at <70°C for $2h$ to form a gel then heated at 100°C over 2 days or 165°C for $1h$. The foam can be fabricated by stirring at <70°C for $45min$, decanting unreacted $KAuCl_4$ solution, rinsing with Millipore water, and stirred in water heated to >70°C until PDMS is cured [19].

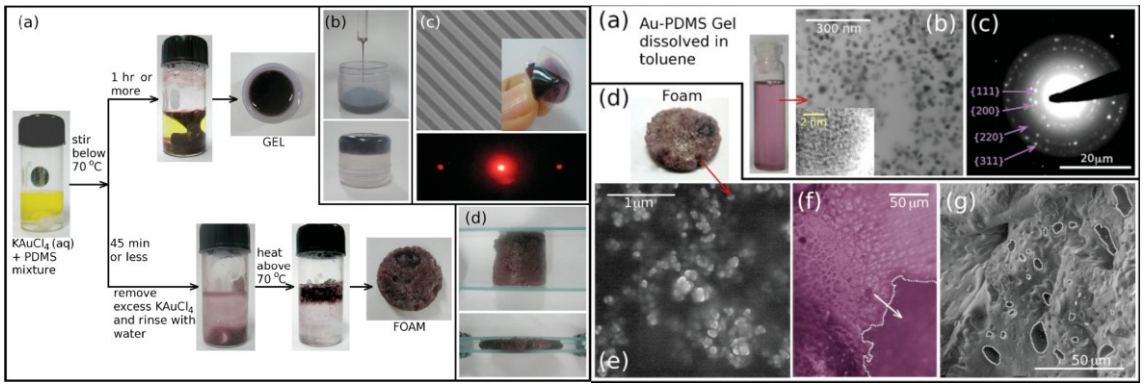

Figure 12: (left) Schematic of PDMS Au NP gel and foam fabrication; and (right) characterization of PDMS Au foam (g inset) SEM of microporous structure. Reproduced with permissions from John Wiley and Sons [19].

TEM of the gel dissolved in toluene indicated the formation of 5-50nm NP crystals. SEM of pores indicate 100-1000μm voids with 10-100μm pitting. It was determined that the NP loading was controlled via the $KAuCl_4$ concentration while the NP incorporation concentration into PDMS was controlled by curing temperature [19].

Salt Fusion Pre-treatment

Solid porogen fusion prior to continuous polymer matrix formation via SCPL and gas foaming process involving compression under CO_2 environment until equilibrium before a quick release of pressure causing polymer foaming and fusion was investigated by Murphy et al. [20].

A modification to the standard SCPL method was completed, where the fused solvated polymer is poured into the moulded fused salt mass. The salt templates were created by exposure in 95% humidity for 0-24h durations in SCPL templating. Compression moulded PLGA and 250-425μm diameter salt dry mix was similarly treated to humidity before being pressurized in CO_2 for gas foaming technique. All moulds were then dried over 2 days in a vacuum desiccator [20].

The resulting high interconnection (holes in the walls of the scaffolding) of the template assists cell migration, ease cell-cell interactions, and improves neural/vascular growth within tissue scaffold. The control of hole diameter and sphericity by salt fusion treatment increases the compression modulus of SCPL

samples. This porogen “caking” phenomenon is seen by the salt surface roughening in Figure 13 and the simplified schematic of Figure 14 as the granules fuse into one another.

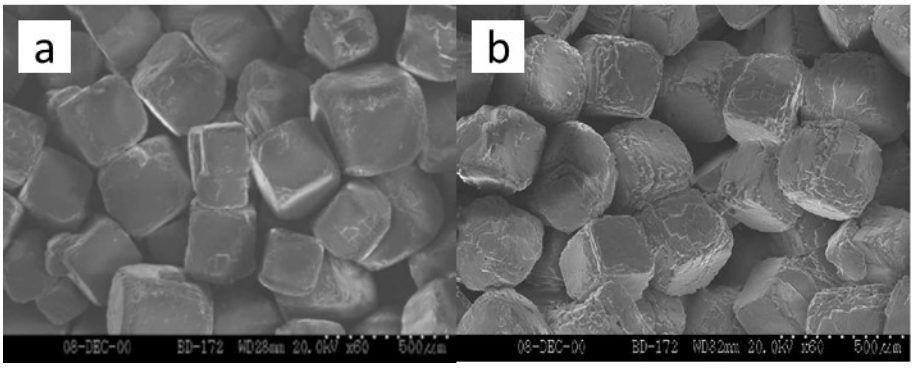

Figure 13: SEM of 95% relative humidity controlled salt fusion at (s) 12h; and (b) 24h. Reproduced with permissions from Mary Ann Liebert, Inc. [20].

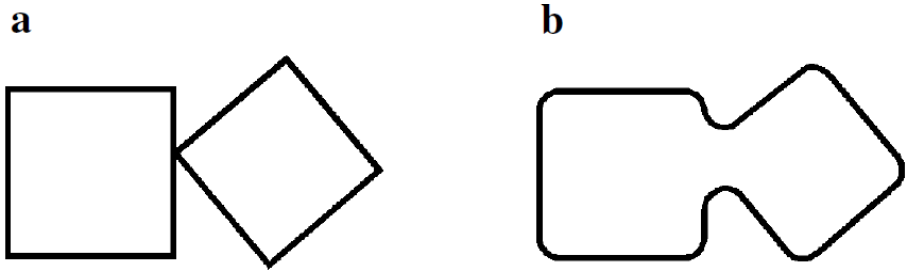

Figure 14: Schematic of salt fusion process at 95% humidity; (a) the granule at the beginning of the process (b) fuses with thick salt bridges after 24h of exposure resulting in salt interconnection. Reproduced with permissions from Mary Ann Liebert, Inc. [20].

The resulting salt fusion pre-treatment increases the elastic modulus of SCPL samples of 97±1% porosity foam and a decrease is modulus for gas foaming samples of 94±1% porosity [20]. This improvement in interconnection and modulus has the potential to promote growth of tissues for tissue engineering applications. In the case of SCPL, the thick struts can improve the structural integrity of the material while the gas foaming method is restricted by the presence of PLGA particles blocking salt fusion. Figure 15 shows the thicker walls of the SCPL method compared to the gas foaming technique.

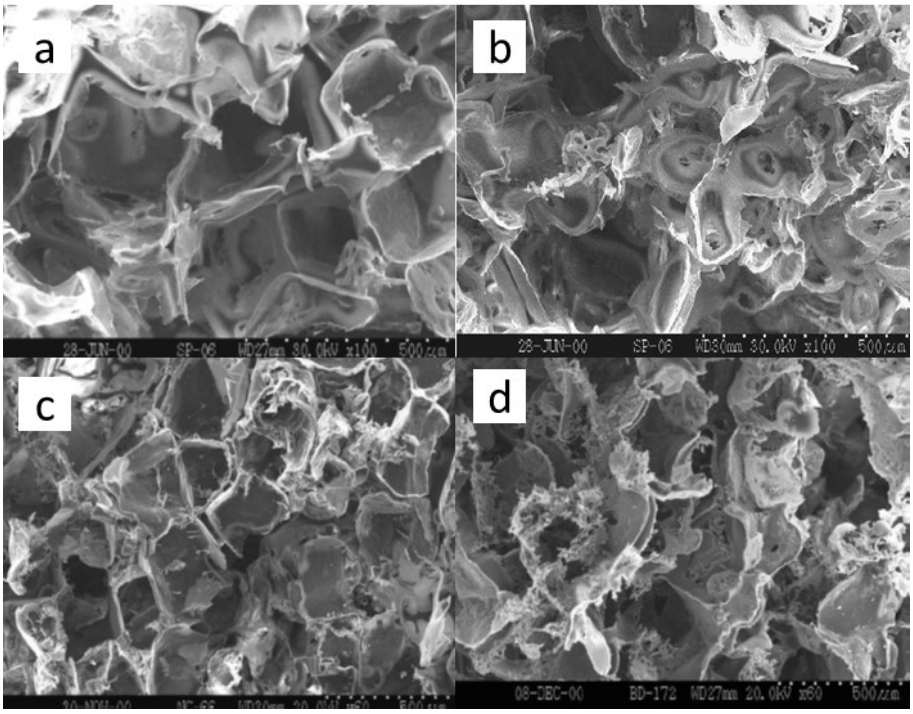

Figure 15: SEM of SCPL PLGA from (a) 1h and (b) 24h salt fused template; and gas foamed PLGA from (c) 1h and (d) 24h salt fused template. Reproduced with permissions from Mary Ann Liebert, Inc. [20].

Sugar Cube Templating

Sugar production has a long history, its packaging form comes in a variety of forms: loose granules, sugar loaf, sugar cube/lump, and sugar cubes. Existing industrial machines and processes have created sugar for ease of handling. The process of moulding and casting itself is also an old invention, providing flexibility in shape and material choice. The use of casting has allowed the mass production and modular component assembly of various machinery and devices. Combining two historical processes together can create a fast and easy implementation of fabricating reusable polymer sponges [21].

Choi et al. uses PDMS, sugar cubes, granular sugar (400-500μm), sanding sugar (1000-1100μm), and black sugar (1500-1800μm) as seen in Figure 16 to fabricate polymer sponges. Sugar is first moulded before immersion in a 1:10 PDMS to crosslinker polymer mixture. After 4h of degassing to promote capillary force infiltration, the sample was cured at 120°C for 12min. Ultrasonic cleaning is completed at 40°C to remove the sugar before air drying [21].

It can be seen in both Figure 16 and Figure 17 the absorption of oil (red) into the PDMS cube while water is repelled. The sponge is reusable and simple to fabricate using sugar as a template. Choi et al. discovered that the sugar granule size can affect the absorption capacity of the PDMS sponge. Figure 16 (b) shows the increase in absorption capacity of transformer oil using various sugar granule sized template.

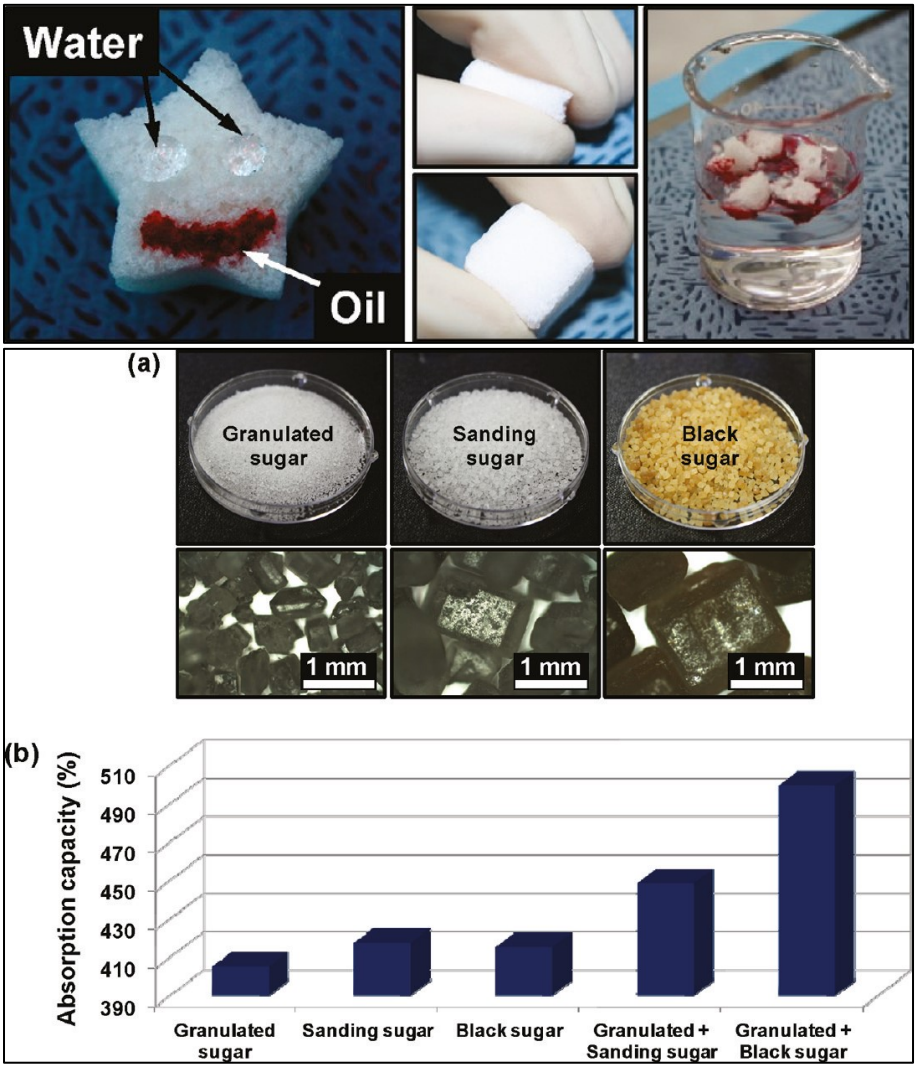

Figure 16: (top) Star shaped oleophilic (red liquid) and hydrophobic (transparent liquid) PDMS sponge; (a) photos of granulated, sanding, and black sugar granules and their microscope images; and (b) transformer oil absorption capacity of PDMS sponges created using different sugar granule sizes. Reproduced with permissions from American Chemical Society [21].

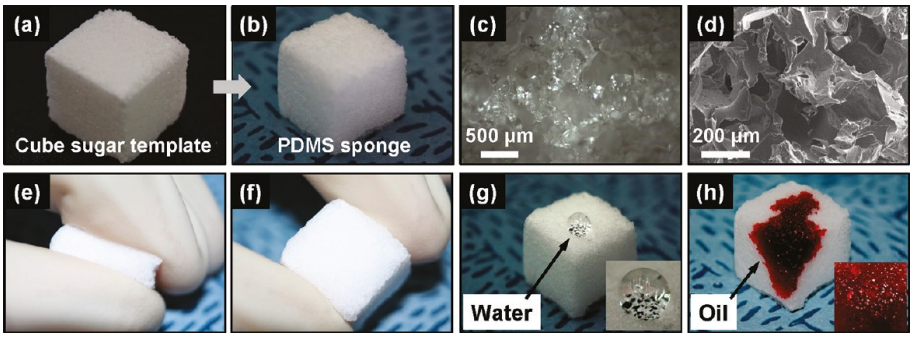

Figure 17: Photograph of (a) sugar template resulting in moulded (b) PDMS sponge; (c) optical and (d) SEM imaging of PDMS sponge; (e, f) photos of PDMS sponge compression, (g) hydrophobic, and (h) oleophilic behaviour. Reproduced with permissions from American Chemical Society [21].

Various oil and solvent capacities are reported and the PDMS cube was found to float atop the water, thus making oil spill clean-up simple without the need of dispersion agent or burning while secondary pollution can be avoided by reusing the PDMS sponges repeatedly. The criteria for oil spill clean-up are selective, fast adsorption, and high capacity. PDMS sponge's reusability and recyclability, reduces cost and its high absorption capacity (several times its weight), and hydrophobic nature makes it an ideal oil absorbent.

Salt Templated PDMS Plug

SCPL technique was used to fabricate a PDMS plug to block tube leaks. Control of the porous structure was achieved via control of PDMS to dimethicone ratio and salt particle size. Exploiting the swelling of PDMS sponges when absorbing organic liquids, it can be used as an expandable stopper [22].

Fabrication of sponges, as seen in Figure 18, used a premix at 10:1 PDMS to curing agent, followed by dimethicone dilution and moulding in a $5mL$ plastic tube, $5min$ of stirring of NaCl 1:1 w/w to PDMS with centrifugation at $8000rpm$ for $20min$, decanting of supernatant, the wet precipitate is cured at $80°C$ for $15h$. Ethanol was used to wash any dimethicone residue, followed by a $40°C$ water soak, dichloromethane and ethanol with manual squeezing was done to remove the salt before drying at $60°C$ [22].

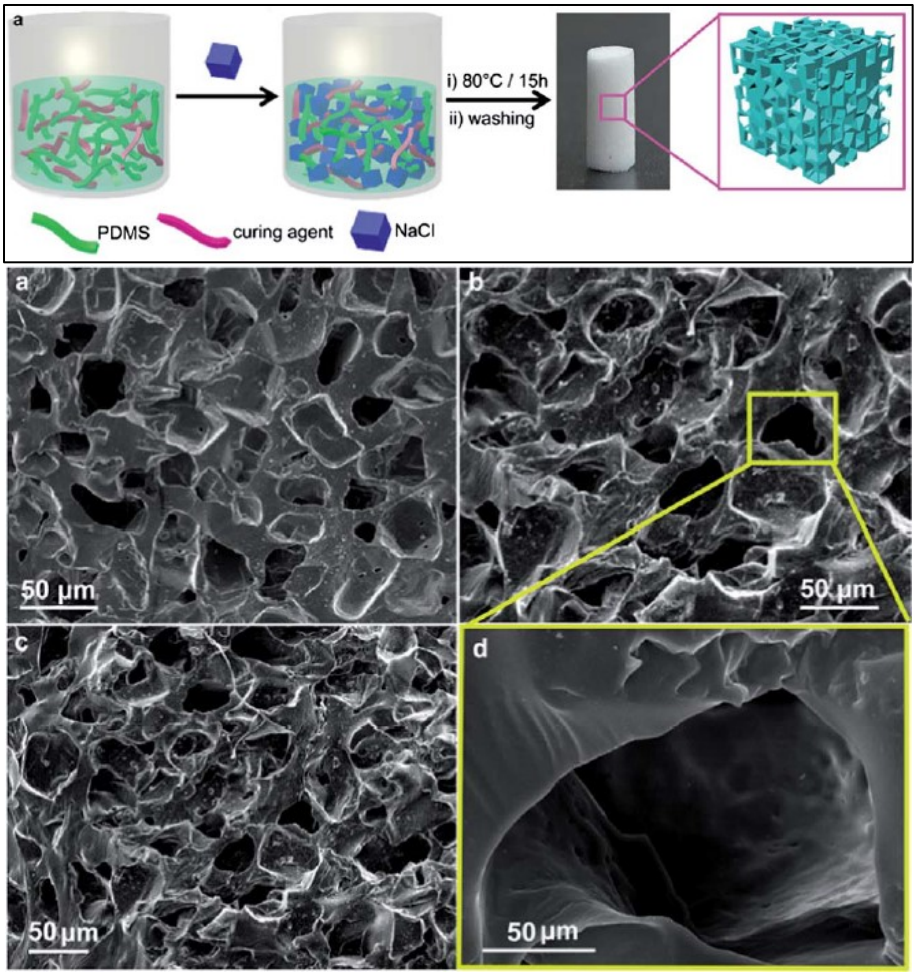

Figure 18: PDMS sponge plug (top) fabrication schematic; and (bottom) SEM imaging of porous material. Reproduced with permissions from Royal Society of Chemistry [22].

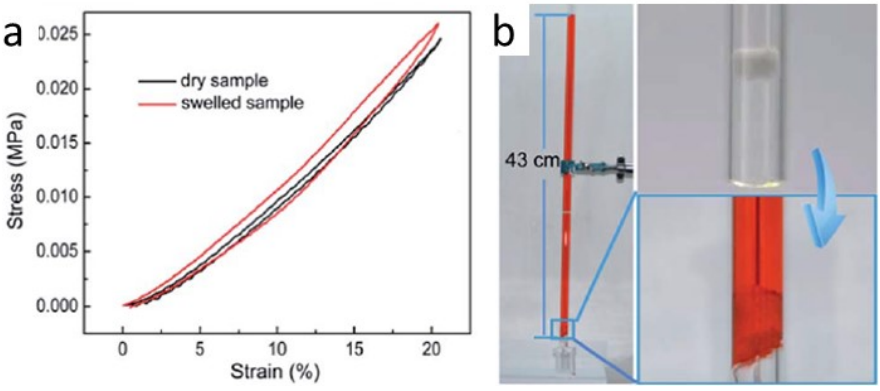

Figure 19: PDMS sponge plug (a) stress-strain curve and (b) plug in 8mm inner diameter glass tube holding 43cm column of n-hexane. Reproduced with permissions from Royal Society of Chemistry [22].

The PDMS sponge plug was evaluated using Oil Red O dyed n-hexane within a glass tube with $7mm$ diameter by $3mm$ thick cylindrical plug. Figure 19 shows the PDMS sponge swell to stop the flow.

Graphene Modified PDMS Sponge: Selective Continuous Absorption

Tran et al. used sugar templating method (on sugar cones) to cast their graphene modified PDMS suction device. This "attachment" is shown to be able to continuously and selectively remove water contaminants when connected to a pump [23].

Fabrication of the continuous flow stoppers used 10:1 PDMS to curing agent polymer premix and the sugar cone was added and degassed in vacuum for $1h$. The wet PDMS was cured at $120°C$ for $12min$ and once cooled, the sugar was leached in sonicating water at $35°C$ for 30-60min. Graphene modified PDMS sponges were prepared by injection of solvent dispersed graphene solution at $50mg$ graphene powder to $20mL$ solvent which underwent $15min$ sonication. The composite sponge was air dried and the process repeated thrice [23]. Resulting testing in Figure 20 showed faster contaminate adsorption of graphene modified PDMS sponges than virgin PDMS sponge as well as demonstrated the continuous flow device in Figure 21.

Continuous vacuum adsorption capacity at $4.5L$ of hexane in $30min$ in a non-turbulent mixture with water using a $55mm$ sponge head before a decrease in efficiency is seen [23]. To simulate realistic conditions, artificial turbulence was created via stirring and the assembly is still able to remove the hexane droplets from emulsion very quickly.

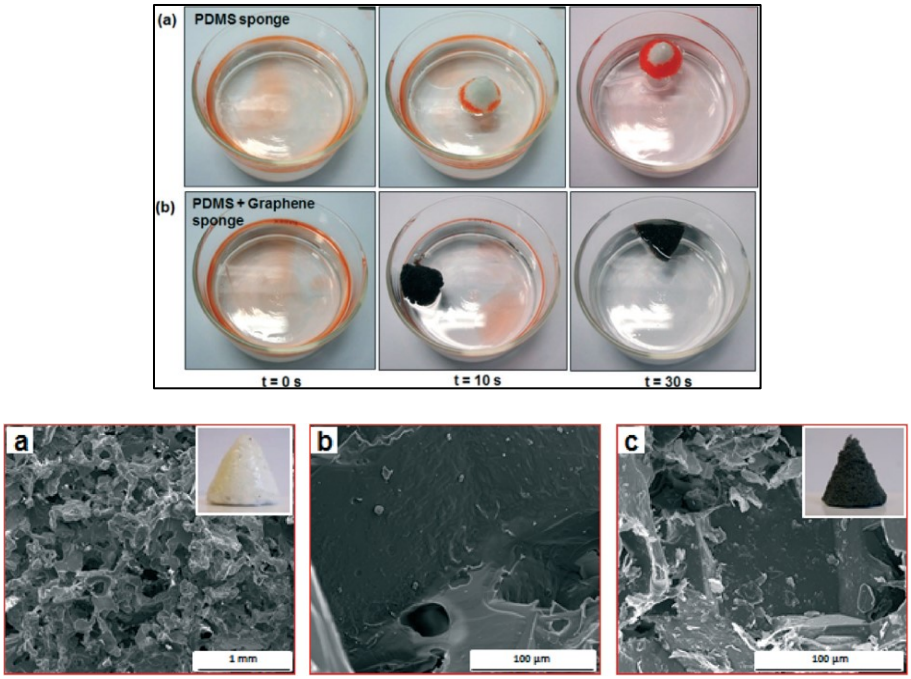

Figure 20: (top) Comparison of (a) PDMS and (b) PDMS-graphene sponge gasoline (orange) adsorption at 0, 10, and 30s; and (bottom) SEM images of (a, b) PDMS and (c) PDMS-graphene sponges. Reproduced with permissions from Royal Society of Chemistry [23].

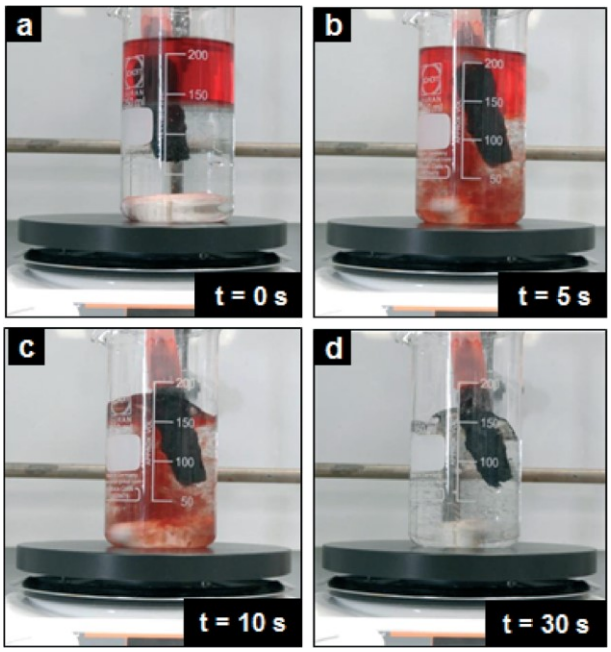

Figure 21: Continuous removal of hexane (red) from a stirring mixture: at (a) onset, (b) 5s, (c) 10s, and (d) 30s of operation. Reproduced with permissions from Royal Society of Chemistry [23].

1.3.2. PDMS Sponge and Foam

PDMS is a transparent, inert, non-toxic, biocompatible, flexible, and non-flammable material. It is used as an antifoaming agent, for medical devices, as a building material, and in soft lithographic applications. PDMS has a viscoelastic behaviour and is hydrophobic, plasma oxidation can modify the surface to exhibit an oxidized surface allowing hydrophilic characteristics.

Publication in PDMS foam is still relatively new. The terms "PDMS foam" and "PDMS sponges" were searched using Google Scholar and the results are presented in Figure 22. The research in PDMS foam/sponge is centred around its adsorption applications. This thesis will explore its use as a dry adhesive backing material.

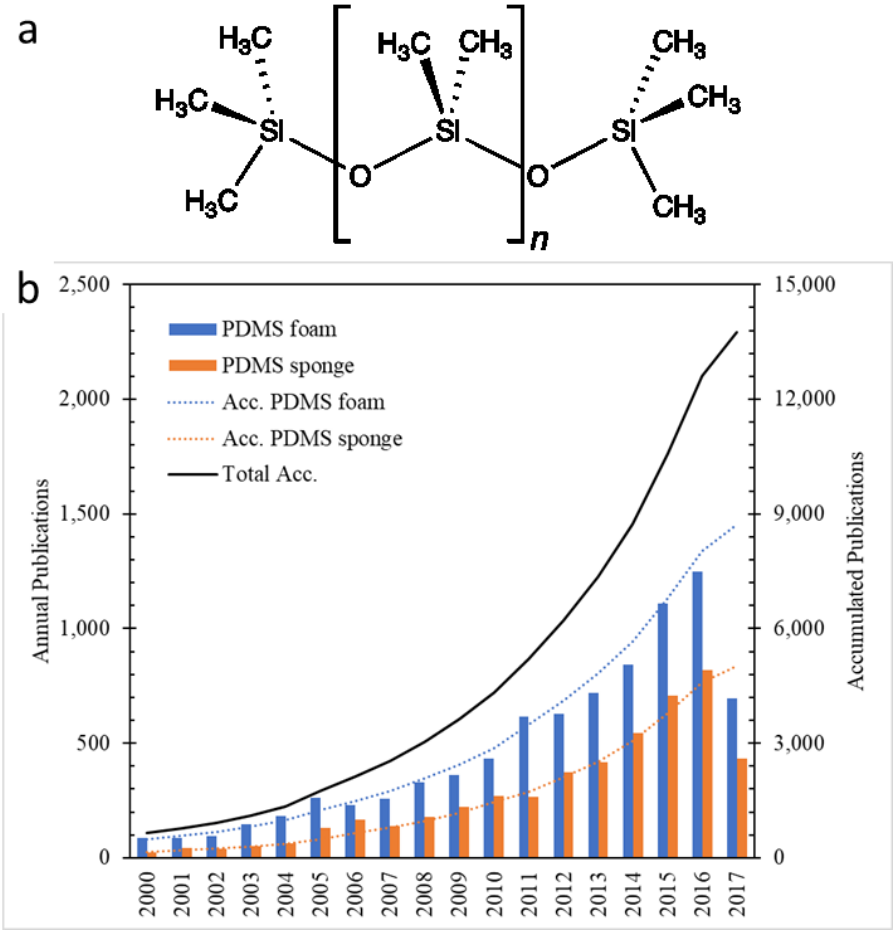

Figure 22: (a) Schematic of PDMS polymer, credits: Smokefoot reuse under public domain (b) number of PDMS foam/sponge publications per year as of June 20th, 2017

Chapter 2. Effect of Foam Backing Material Thickness on Adhesive Properties at Low Preloads [1]

A myriad of natural substances have outstanding bulk resistance to cracking, deformation, and damage, due to their micro-structured or porous gradations [5], [24], [25]. These materials are composed of stress bearing structures orientated in the direction of force. Common examples of such materials can be found in bamboos, bones, plant stems, and squid beaks [24]. The fully hydrated Humboldt squid's beak embedded in its soft buccal envelop, generates a chemical gradient which results in a stiffness ranging two orders of magnitude across its entire structure [25]. FGM are deemed engineered mimics of their natural analogues, synthetically manipulating and redistributing the stress and strain experienced by the material [24].

Interestingly, bioinspired fibrillar adhesive systems of some animals and insects such as geckos and spiders have long been regarded as graded materials. In addition to their sophisticated surface geometry, the underlying mechanism of such biological adhesive systems relies on the graded structural and mechanical properties of their surface and backing layers. Both theoretical and experimental studies have shown that fibrillar dry adhesives are robust and flaw tolerant due to the graded nature and high compliance of its fibrillar structures and backing layers [5], [11]. Numerous types of wet and dry adhesive systems have been developed, ranging from simple polymer blocks to mushroom shaped and film-terminated micropillars, bundled into single or multi-level hierarchies using conventional nano/microfabrication techniques [5], [9], [26]–[33]. These structures have different adhesion behaviours, dependent on the nature of their mechanically graded fibrils and backing layer along its thickness.

Despite great achievements in the manipulation of adhesion through geometric surface alterations [34], [35], the contribution of soft backing materials on these properties have received less attention and only a limited number of publications address the systematic study of gradient mechanical properties along the thickness [36]. Inspired by the graded nature of gecko and tree frog toe pads, a biomimetic FGA system using film-terminated PDMS micropillars was developed by our group, simulating the soft organic tissue

beneath. The outstanding adhesive properties of these structures was found to be attributed to the compliant nature of the backing material [5]. A new dry adhesive is proposed in this work, using a single-layer foam backing layer with a terminal thin film to take advantage of the high energy absorption characteristics of cellular materials, that usually experience stress-plateau during compression, absorbing a large amount of energy during deformation [37], [38]. Polymer foams, as a class of cellular materials, are used in dry adhesive systems due to its superior energy absorption capability, resulting in high adhesion with the surface. The dependence of adhesive strength on foam layer thickness and preload was investigated. Additionally, the film-terminated foam-based adhesive demonstrates a simpler and less expensive alternative to the current complex fabrication process of dry fibrillar adhesives. As an example of an application of this material, the adhesive pad was employed in the transportation of delicate objects.

2.1. Materials and Methods

2.1.1. Fabrication of Thin Film Terminated Foam Adhesives

The steps involved in the fabrication of a film-terminated foam-based adhesive sample are illustrated in Figure 23. A mixture of PDMS (Sylgard 184, Dow Corning) at 10:1 weight ratio of resin to curing agent were prepared, vortex mixed, and vacuum degassed before being used in subsequent steps. The terminal film and foam backing were fabricated separately before fusing together to avoid defects, ensuring a high quality terminal films.

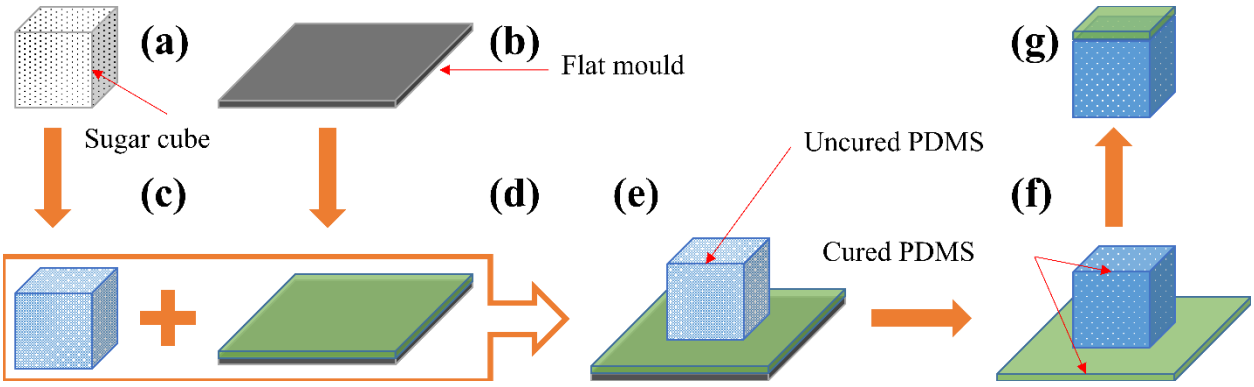

Figure 23: Fabrication schematic of film terminated silicone foam adhesive: (a) sugar cube template; (b) flat silicon wafer; (c) PDMS soaked sugar cube; (d) cured PDMS thin film; (e) uncured PDMS soaked

sugar cube placed on cured PDMS film; (f) PDMS soaked sugar cube cured, sugar removed, and system is peeled from mould; (g) finished film terminated foam dry adhesive system.

First, the terminal thin film was fabricated by pouring $2g$ of PDMS premix onto a pre-treated flat <100> p-type silicon wafer (University Wafer) and spin-coated (Specialty Coating Systems G3-8) at $3500rpm$ for $45s$, rested for $5min$, and cured at $120°C$ for $1h$. All foam samples had a terminal film fabricated in this manner. Second, the sugar cube template was placed into a petri dish of PDMS premix and degassed for 1-2h to displace the air within the template with polymer liquid. Excess liquid was scrapped from the sides of the polymer soaked sugar cubes using a straight edge. The wet uncured cube was placed directly onto the cured film still attached to the silicon wafer. The cube was left to rest for $5min$ with a small weight on its top face before being cured at $120°C$ for $2h$. After cooling, the film terminated cube was detached from the silicon wafer and any polymer flashing was trimmed. The thickness of the sugar-polymer system was adjusted by polishing the cube against a sandpaper block until the desired values of 5 and $10mm$ were reached. The native dimension of the sugar-polymer system is approximately $15mm$.

Finally, the sugar-polymer system was placed into a container of DI water and sonicated for $2h$ resulting in the dissolution of sugar, removing the template. The film-terminated foam was then dried in the oven at $120°C$ overnight to remove any residual water. The polymer control sample was fabricated by pouring the premix formulation into a petri dish and cured alongside the foam samples to avoid variations in curing conditions, sample thicknesses varied from 1.5-3.0mm which did not affect the pull-off force. Four samples of each foam thickness were fabricated and for brevity and clarity, we designate the samples by the type of backing material i.e. “f XX”: film terminated foam sample, where XX is the thickness of the foam in millimetres and “C”: polymer block control. The sample name may be followed by “- YY mN”, where YY denotes the preload force.

Silicon wafer pre-treatment was completed to aid PDMS thin film release. 1-2 drops of (heptadecafluoro-1,1,2,2-tetrahydrodecyl) trichlorosilane (FDTS) (Gelest, Inc.) were added to $250mL$ of pentane and the silicon wafers were submerged and left to soak in the solution for $1h$ before rinsing with

pentane and left to dry under airflow. It was followed by curing at $90°C$ for $1h$ and cleaned with KimWipes and ethanol to remove any residue.

2.1.2. Characterization

The adhesive structure is composed of two different components: the film-terminated surface and the backing material. The thickness of terminal film was measured by an optical profilometer (RTEC Instrument) and the porosity of the backing material ($\boldsymbol{\mu}$) was calculated from the density and volume of PDMS and sucrose. Replication of the sugar template was confirmed by SEM of a cross sectional segment of the porous foam.

The same custom-built micro-indentation machine used in our previous work [5], [7] was employed to measure the adhesive properties of the fabricated samples. Indentation tests were carried out with different preload forces of: 0.1, 1, 5, and $10mN$, using a $6mm$ diameter hemispherical glass probe (ISP Optics Corp.) attached to a flat and levelled glass slide. A single $7mN$ preload test profile was later added for each sample to confirm their trends. Every sample had its foam end attached to a 1/2" slotted head, 1/8" pin SEM aluminium stub (Ted Pella, Inc.) using double sided tape. The approaching and retracting velocities were set at $1\mu m/s$ with $1s$ holding time between them. Tests were completed in ambient temperature and humidity. At least *three* locations on each sample were tested and their average preload and pull-off values are reported with error bars. Tests were performed in the same day alongside a flat PDMS block as control. KimWipe and ethanol was used to clean the glass probe and remove debris/fibres from the sample film terminated end, followed by air drying, prior to testing.

A universal mechanical tester (UMT) (Centre for Tribology Inc.) was employed and manually controlled for the pick and place demonstration using a $100kg$ load-cell with a clamp attachment.

2.2. Results and Discussion

2.2.1. Structure of Thin Film Terminated Foam Adhesive

PDMS foams are commonly used in the production and development of re-useable water remediation materials [21]–[23], [39], [40]. In this work, we proposed to use the PDMS foam as a backing

material to enhance the compliance and adhesion of the elastomer film. The foam structures can be fabricated using various methods involving a sacrificial template to control porosity. Using loose and fused grains of commonly available water soluble solids such as salt [18], [20] and sugar [21]–[23], [39], [40] are fairly popular. Herein, the sugar cube templating method was selected due to its uniform and consistent dimensionality and porosity for fast prototyping and modular design. Figure 24(a) shows the similarity of the sugar cube template and completed film terminated foam adhesive. Figure 24(b) shows an image of the cured system where the terminal film is completely transparent, exposing the granular structure of the foam material behind it. Figure 24(c) is a SEM image of the terminal film surface after several uses prior to cleaning. There is some accumulation of particulate debris and fibrous material. This image also highlights an area of defects on the film, as seen by the pore pitting. This defect is suspected to be from imperfect contact between the terminal film and backing layer, likely due to some trapped air pocket at the interface during the fabrication process. Figure 24(d) is a SEM image showing the overall structure of the sacrificial sugar cube template perfectly replicated in the PDMS foams. The foam has a continuous porous structure and the imprints left by the sugar template can still be seen with its regular crystalline geometry.

The dimensions of the sugar template were measured (n=20) to be: 15.63$\pm$0.07 by 15.55$\pm$0.09 by 15.56$\pm$0.14mm, having a mass of 3.5261$\pm$0.0239g. The sugar cube's porosity was calculated using the density of sucrose (1.587$g/cm3$) to be: 41.23$\pm$0.77%. After removal of the sugar, the polymer foam's porosity was calculated using the specific gravity of PDMS (1.03 at 25°C) to be: 70.62$\pm$1.78% which is larger than the expected porosity (~58.77%) from the sugar cube. This discrepancy in foam porosity may be attributed to incomplete absorption of PDMS into the sugar template prior to curing or the sugar cube may have inaccessible voids where PDMS is unable to penetrate due to air pocket trapping or sugar crystal grain volume exclusion. The relative density of the foam is calculated from $\boldsymbol{\varphi_0 = 1 - \mu = \frac{\rho}{\rho_s}}$ where $\boldsymbol{\mu}$ is the porosity of the foam, $\boldsymbol{\rho}$ is the density of the foam, and $\boldsymbol{\rho_s}$ is the density of the constituent material. The relative density was found to be ~0.3, which classifies the structure as a high-density foam.

Previous studies on elastic film-terminated fibrillar interfaces has shown a slight increment of the energy release rate with a decrease in the thickness of the terminal layer, $\boldsymbol{t^3}$, where $\boldsymbol{t}$ is the thickness of the terminal layer [5]. The proposed film-terminated foam structure resembles a film-terminated fibrillar interface due to the supporting cellular walls of the foam. Therefore, it is reasonable to anticipate similar dependency of the adhesion to the film thickness. However, the fabrication and peeling of very thin terminal films can damage the terminal film. Thus, preliminary work in this study showed that the defect-free terminal layer of thickness of $19.10 \pm 0.37 \mu m$ can be attached to the foam samples.

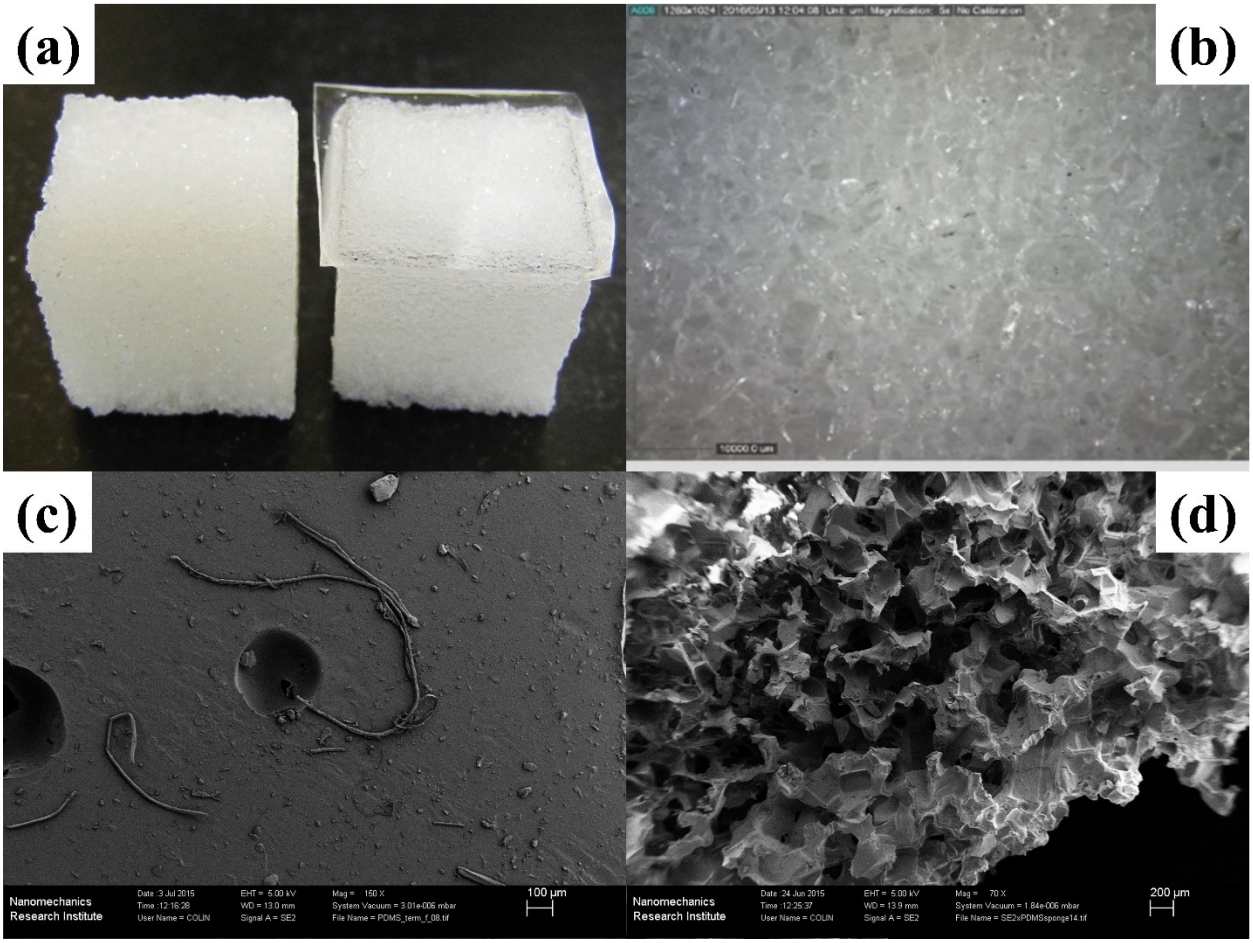

Figure 24: (a) Close-up image of (left) sugar cube and (right) film terminate PDMS foam adhesive cube; (b) A top-view optical photo of the film-terminated foam cube showing the transparent film and granular foam structure behind it; (c) SEM image of the terminal film after several uses, showing accumulated

particulate and fibre contaminants along with pore pit defects; (d) SEM image of the PDMS foam showing sacrificial sugar crystal imprint and the continuous porous void

2.2.2. Adhesion Behaviour of the Film-Terminated Foam Samples

Indentation experiments, setup as seen in Figure 25(a), were performed to investigate the adhesive behaviour of the film-terminated foams. As expected, indentation test on the flat control samples of PDMS with different thickness resulted in similar adhesion behaviour. Therefore, adhesion of the control sample can be deemed thickness independent within our millimetre test range. Figure 25(b) illustrates an example load-displacement curve for the PDMS flat control and film-terminated foam adhesive, "f10".

The approaching snap-in force were trivial for both control and foam samples. The normal compressive loading progressed till a fixed preload of $10mN$. The maximum indentation depth reached in all experiments was <$100\mu m$ which is far below the dimensions of the probe. The slope of the loading portion of load-displacement curve lower for the foam sample compared to the control sample, indicating a drastic softening at the interface contributed by the foam backing material. The notable difference in the surface stiffness ($\boldsymbol{S = dF/d\delta}$), i.e. the slope of the unloading portion and the surface compliance ($\boldsymbol{C = 1/S = d\delta/dF}$) can be readily observed. The slope of loading and unloading portion of the indentation curves for the control sample are similar due to small hysteresis, while the foam sample undergoes great hysteresis during unloading as can be seen by the difference in slope of the loading and unloading portions. Retraction continued until the pull-off point is reached, where the tensile adhesive force is at a maximum. It is apparent that the addition of a foam layer as the backing material enhances the pull-off force of the simple flat control PDMS sample. The de-bonding for both samples is rather smooth and fast without the common crack trapping mechanism usually observed in film-terminated fibrillar adhesives [5], [41]. Visual post-inspection of the foam-based adhesive showed no defect marks left post indentation, essential for reusability.

Two adhesion descriptors: pull-off force ($\boldsymbol{F_{max}}$) and the overall work of adhesion ($\boldsymbol{W_{adh}}$), were used to quantitatively compare the adhesion of the proposed PDMS foam-based adhesive with the flat

control. The variation in effective elastic modulus of the foam along the thickness was also estimated from the indentation curves to verify the graded nature of the foam adhesive.

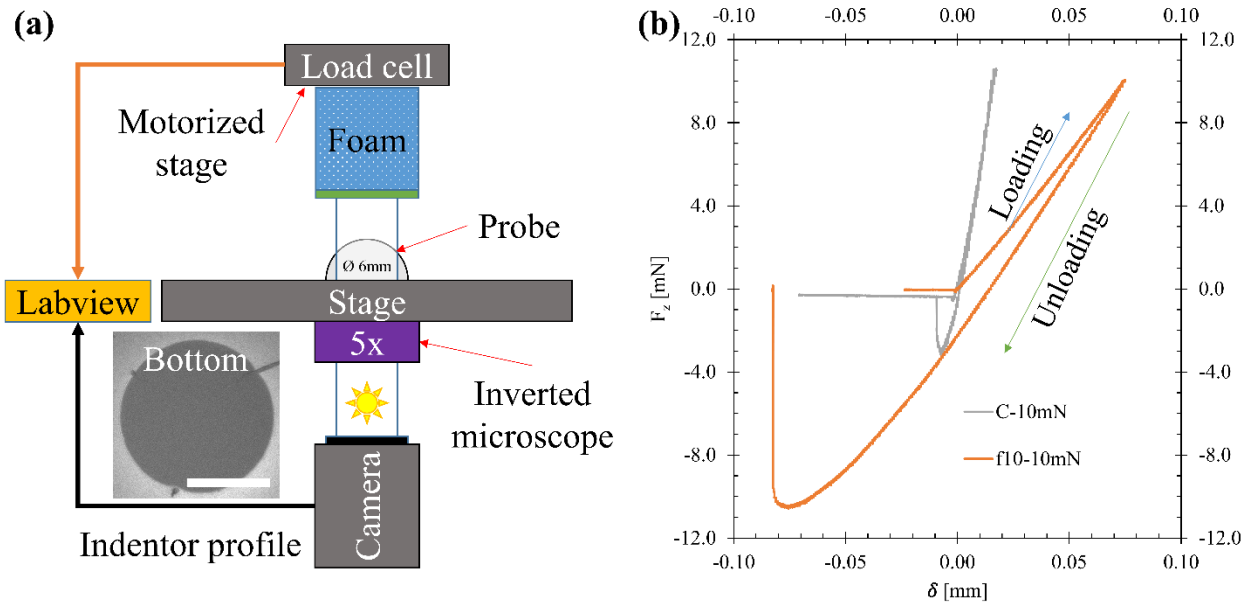

Figure 25: (a) Schematic of foam indentation test setup with sample bottom view contact area (scale bar at 200μm); (b) typical force (F_z)-displacement (δ) indentation curve of the control sample "C-10mN" and film terminated foam "f10-10mN" with the same preload

The influence of foam thickness and preload on pull-off force are shown in Figure 26(a). It is observed that the pull-off force reaches optimal values at around $10mm$ foam thickness before decreasing slightly for $15mm$ in the preload range of 0.1-$10mN$. The cause of this decrease is still unknown and will be subject to future study. However, the increasing trend in pull-off force with the foam thickness can be attributed to the ratio of the contact radius to foam thickness, i.e. the confinement parameter ($\boldsymbol{a/h}$), and its effect on the compliance of the samples. To obtain more insight about the physical properties of our system, we assume that the contact mechanics of soft elastic bodies can be used to interpret our results. The compressive deformation of an elastomeric cellular material usually starts with a linearly elastic region, followed by the non-linear elastic buckling of the cells, and eventual collapse of the cells causing a drastic rise in stiffness. Our assumption is reasonable as, at the low preload range of 0.1-$10mN$, our foam-based adhesives showed linearly elastic behaviour.

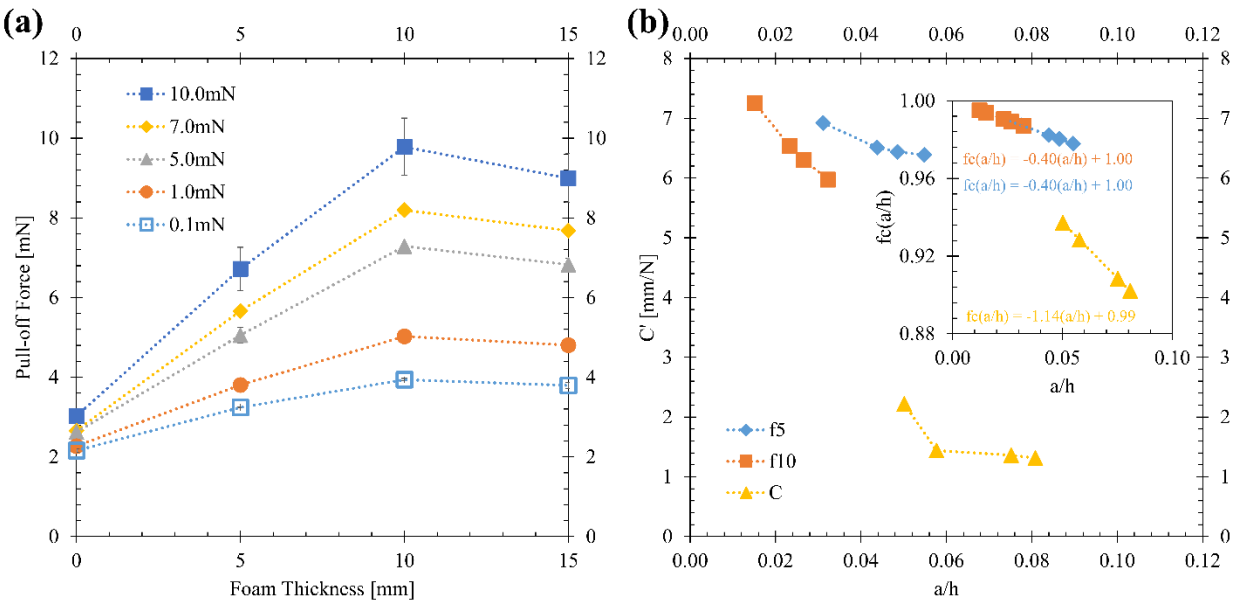

Figure 26: (a) Pull-off force vs. foam thickness for various preloads; (b) compliance vs. a/h of control and 5 and 10mm foam adhesive system (inset) $f_c(a\ /\ h)$, correction factor fitting

It is known that the ratio between the contact radius and thickness of an elastic half-space subjected to a normal compressive force affects the actual value of the normal displacement and compliance [42]. The compressive force, displacement, and compliance of the contact between a rigid hemispherical probe and a soft elastic half-space with infinite thickness ($\boldsymbol{a/h \rightarrow 0}$), whether obtained in the framework of Hertz or JKR contact mechanics, will be unaffected by the confinement ratio. This is not the case for a soft half-space with finite thickness, where the confinement ratio increases. Shull has introduced geometrical correction factors for all mentioned parameters to account for finite systems. The effective compliance ($\boldsymbol{C'}$) is obtained by considering the geometrical correction factor ($\boldsymbol{f_c}$):

$$\boldsymbol{C' = C f_c\left(a/h\right)};\ \frac{\mathbf{1}}{\boldsymbol{f_c(a/h)}} = \mathbf{1} + \left(\frac{\mathbf{0.75}}{\boldsymbol{((a/h) + (a/h)^3)}} + \frac{\mathbf{2.8 * (1 - 2\nu)}}{\boldsymbol{(a/h)}}\right)^{-1}$$

As the contact area is pinned during unloading, the effective modulus of our samples can be calculated using the Boussinesq definition of compliance: $\boldsymbol{C_B = C = \frac{1}{2E^* a}}$ [5], [42], [43], where E^* is the reduced Young's modulus of the soft material defined as $\boldsymbol{\frac{1}{E^*} = \frac{(1-\nu^2)}{E}}$. According to Gibson and Ashby, a

wide class of disordered cellular materials have the initial Poisson's ratio of $\boldsymbol{\nu \approx 0.33}$ [38]. However, the Poisson's ratio of low-density foam rapidly decreases with excessive compressive loads as shown by Zhu et al [44]. In a compression test with strains up to 75%, we found that the Poisson's ratio of our material is approximately ~0.20. The geometrical correction factor can be calculated and compliance of the structures can be determined using the reverse slope of the unloading portion of the indentation curve. Figure 26(b) shows the corrected compliance vs. ($\boldsymbol{a/h}$) of samples "f5" and "f10" for different preloads. The inset graph shows the variation in the calculated correction factor, $\boldsymbol{f_c(a\ /\ h)}$ with the confinement parameter $\boldsymbol{a/h}$. Assuming either frictionless or full-friction boundary conditions will create only marginal errors in the calculation [42]. Thus, it is apparent that the compliance increases with the thickness of the foam backing layer, resulting in larger contact area and pull-off force.

To verify the nature of the foam-based adhesive as a graded material, we determined the variation of elastic modulus versus strain in the direction of the thickness. Figure 27 shows variation of the elastic modulus ($\boldsymbol{E}$) with the maximum strain at preload ($\boldsymbol{\epsilon_{max}}$) of the fabricated samples. Cellular materials are known to soften with increasing compressive deformations until the cell walls begin to come into contact, before gradually increasing in stiffness approaching full bulk density. Thereafter, the modulus of the foam will approach that of the bulk material [45]. The dominant mechanism of deformation for linearly elastic foams is the reversible bending of the cell walls. It has been shown for open-cell foams that the initial tangent modulus can be written as $\boldsymbol{E^c = A_0 E^s [\varphi_0]^2}$ where $\boldsymbol{A_0}$ is a geometric constant of proportionality, $\boldsymbol{E^s}$ is the tangent modulus of the parent solid and $\boldsymbol{\varphi_0}$ is the relative density of the foam [38]. Schraad and Harlow have shown that both the proportionality constant and relative density evolve with strain when the foam is subjected to compression [45]. Therefore, the modulus of the cellular material will be a function of strain as: $\boldsymbol{E(\varepsilon) = A(\varepsilon) E^s\ [\varphi(\varepsilon)]^2}$. The functionality of the proportionality constant and the relative density with strain depends on the loading, geometrical, and material properties, whose detailed study is out of scope of this paper. However, an empirical correlation between modulus and strain of our proposed structure is shown in Figure 27.

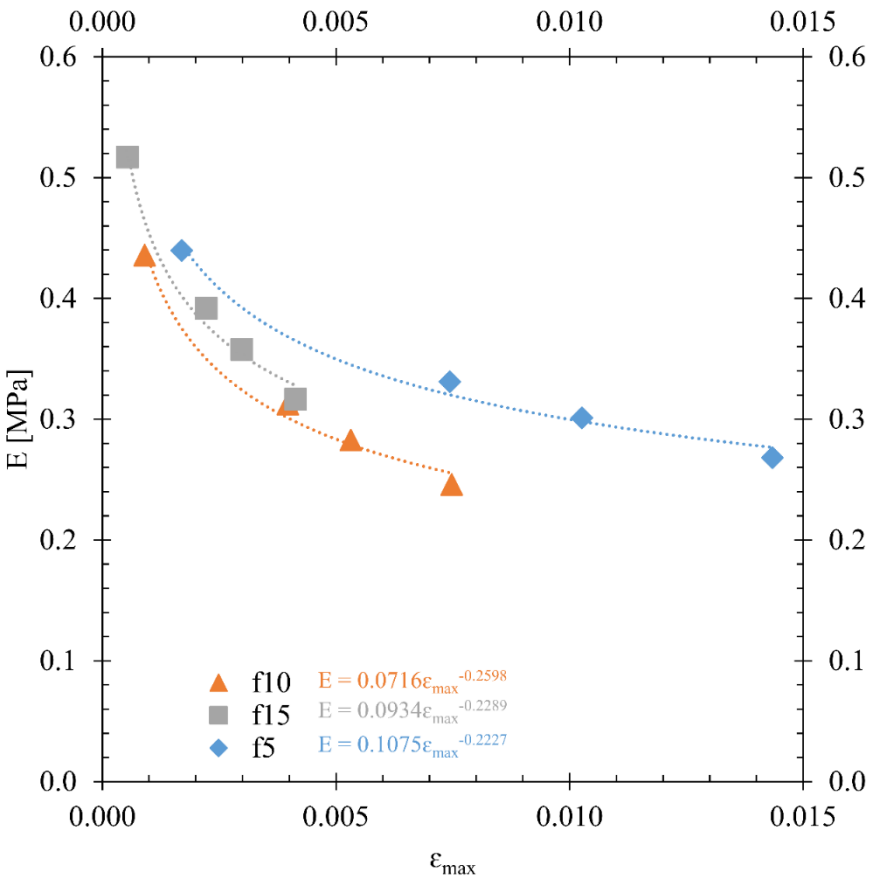

Figure 27: Elastic modulus vs. maximum strain of 5, 10, and 15 mm film terminated foam

The increase in pull-off force with preload is shown in Figure 28. Similar trends have been observed for both elastic and functionally graded biomimetic fibrillar adhesives due to the gradient of mechanical properties along its thickness [5], [46]. It is noteworthy to consider that thickening the foam layer corresponds to enhanced sublayer void fractions in the biomimetic fibrillar adhesive, which can be achieved by increasing the aspect ratio or spacing between the fibrils. Kim et al. have shown that thinner solid and homogenous backing material creates more evenly distributed stress in the contact of fibrillar adhesives, yielding higher pull-off forces [36].

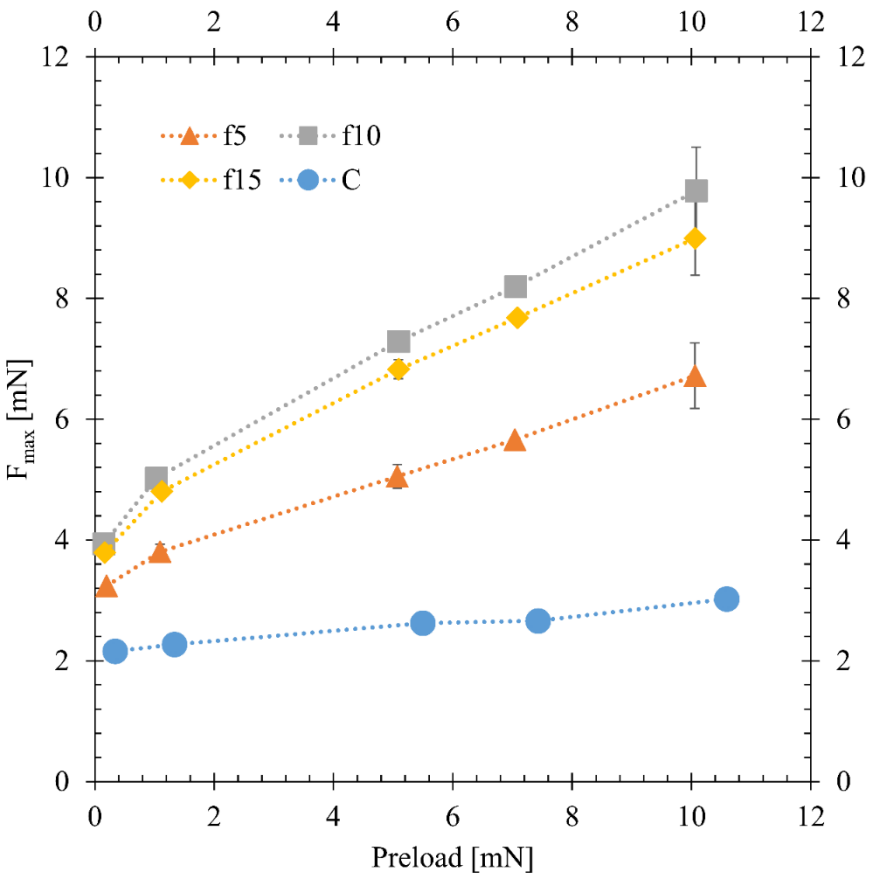

Figure 28: Pull-off force vs. preload for various film terminated foam thicknesses

Another important adhesion descriptor is the overall work of adhesion. In the loading portion of an indentation test, the intermolecular surface attractive forces result in the storage of strain energy, providing the work required for the separation of contact surfaces during unloading. The hysteresis of an adhesive ($\boldsymbol{U_{hys}}$) occurs due to the dissipation of energy in a loading/unloading cycle. The overall work of adhesion ($\boldsymbol{W_{adh}}$) is defined as the hysteresis per change in contact area, an effective adhesion descriptor for PDMS [5], [43], [46], it is defined as: $\boldsymbol{U_{Hys}} = \oint F d\delta$; $\boldsymbol{W_{adh}} = \frac{\boldsymbol{U_{hys}}}{\boldsymbol{A_{max}}} = \frac{\oint F d\delta}{\boldsymbol{A_{max}}}$, where $\boldsymbol{A_{max}}$ is the maximum contact area at the preload holding time. As the indentation tests were performed at different preloads, both $\boldsymbol{A_{max}}$ and $\boldsymbol{U_{hys}}$ vary from test to test. For such a case, the slope of the $\boldsymbol{A_{max}}$ and $\boldsymbol{U_{hys}}$ has been introduced as a reasonable estimate of the overall work of adhesion [5], [46]. Figure 29 shows the linear relationship between the hysteresis and the maximum contact area for the flat control sample, sample "f5", and "f10".

The work of adhesion can be determined from the slope of the fitted linear model. The work of adhesion was calculated to be $0.0898 J/m^2$ for the flat control "C", $1.0951 J/m^2$ for "f5", and $1.8589 J/m^2$ for "f10".

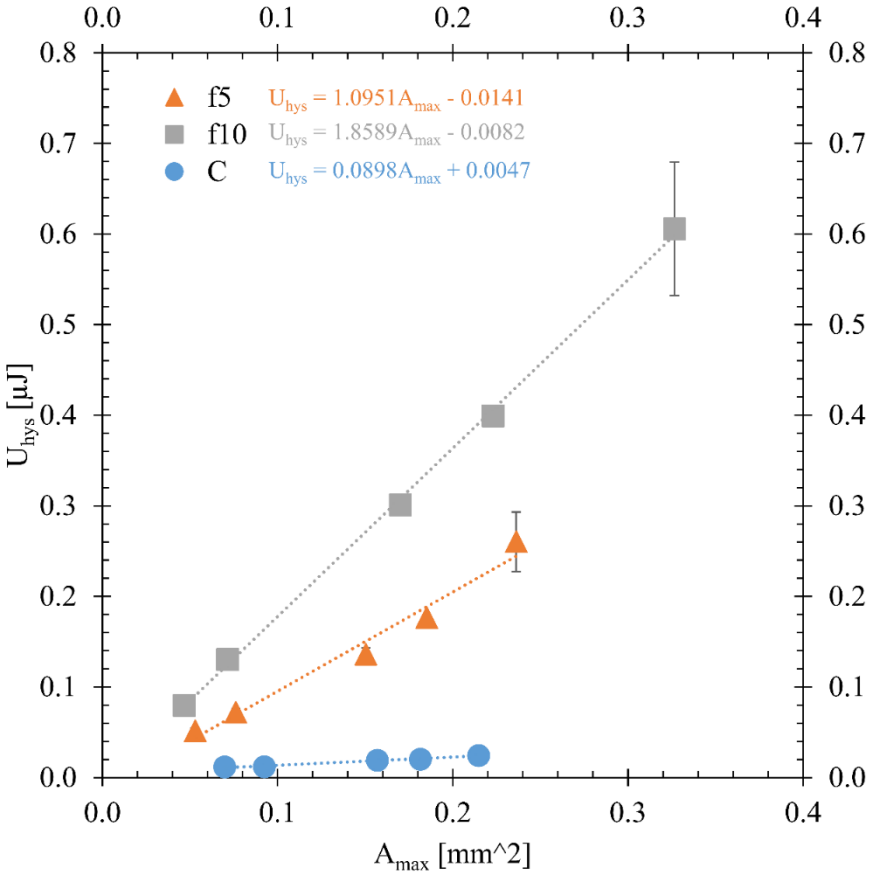

Figure 29: Adhesion hysteresis changes linearly against the maximum contact area. The slope of the lines represents the overall work of adhesion

The results suggest that the use of foam backing enhances the work of adhesion of the flat control sample by almost 20 fold. Interestingly, the work of adhesion of the foam-based adhesive is more than quadruple that of the elastic film-terminated biomimetic fibrillar adhesives ($0.3\text{-}0.4 J/m^2$) reported in previous work [5], [46]. Note that the usual thickness of the backing materials in the aforementioned fibrillar adhesives is around $1 mm$ and thickening the backing material has adverse effect on the adhesion as studied by Kim et al. [36]. As a result, the proposed foam-based dry adhesive may have great potential as a more facile, simpler, and cost-effective fabrication route for the production of dry, reusable adhesives. Although the work of adhesion is lower than that of mushroom shaped micropillars [4], such a simplified and

economic technique can provide great flexibility in the variation of the foam's physical and geometrical parameters that might lead to improved work of adhesion without changing the terminal structures.

2.2.3. Application of Film-Terminated Foam-Based Adhesives as FGAs

Dry biomimetic fibrillar adhesives have been used in emerging technologies such as robotics, micro-manipulation, and in the transport of light objects [27], [47]–[50]. Our proposed adhesive structure benefits from high adhesion strength and repeatable use. There is great potential in applications for the transportation of thin, fragile, and flat materials with reusable foam-based adhesives. Figure 30 shows the transportation of a 4" silicon wafer by a cube of film-terminated foam-based adhesive. The normal compression of the adhesive patch approaching the surface enables the attachment of the object as shown in Figure 30(a-b) with a displacement of $\geq 0.75mm$. The adhesion of the silicon wafer on the foam adhesive remains stable during the vertical and lateral movement of the object as shown in Figure 30(c-e). Interestingly, we found that the adhered object can be readily released using a shear force generated by lateral movement, $\geq 2mm$ displacement when the object is confined in its new location, seen in Figure 30(f-g). The release is triggered by the initiation of a crack on one edge of the adhesive interface, as observed from the left side of the adhesive interface in Figure 30(f); the detailed mechanism of the detachment needs further investigation.

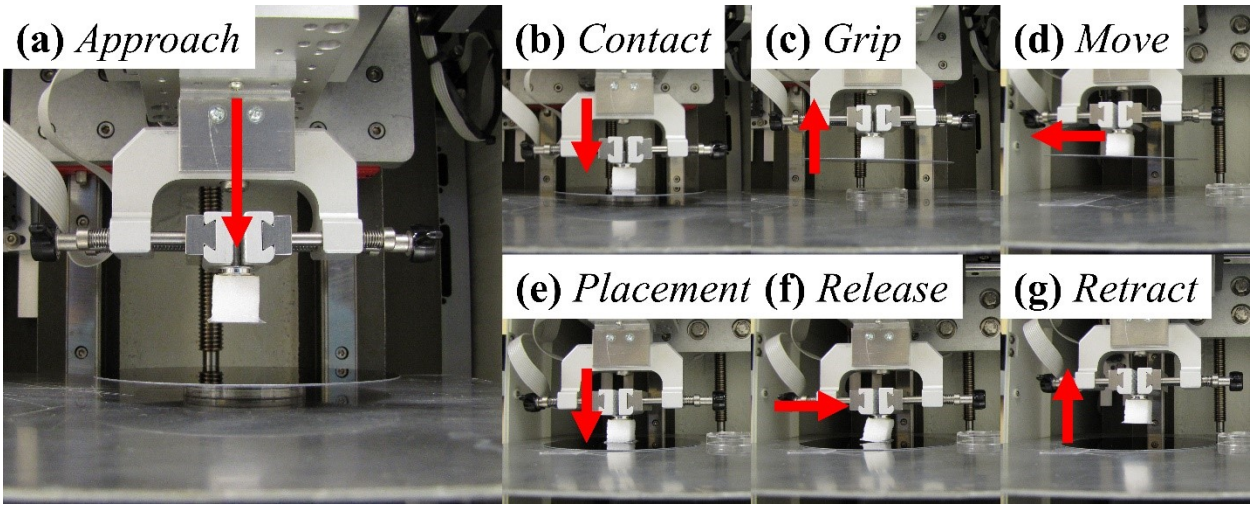

Figure 30: Snapshot of pick and place of film terminated foam using a UMT machine with red arrows indicating the movement of the grip head

2.3. Conclusions

Film-terminated silicone foam has been successfully fabricated and demonstrated to operate as a dry functional graded adhesive. The fabrication of foam adhesive is relatively simple; it can replace current complex, multi-step low-throughput fabrication techniques for fast modular fabrication of gripper heads and mounting pads. The adhesion behaviours of the film terminated foam adhesives were characterized in terms of its compliance, effective modulus, adhesive pull-off force, and work of adhesion. The foam elastomer backing shows remarkable improvement in adhesion performance, thanking to its open cell foam structure which can absorb and dissipate energy. In contrast to the bulk polymer, the adhesion of foam adhesives was found to be preload dependent and increases with preload. Furthermore, the influence of the foam thickness was systematically studied, showing an optimum foam thickness of around $10mm$ for the highest adhesion in the preload range of 0.1-$10mN$. This study was also able to demonstrate the use of such a foam adhesive as a mounting pad for pick and place applications of smooth delicate materials. Since both homogenous foams and FGMs are well-known energy absorbing materials, there seems to be great potential in the utilization of the energy absorption properties of functionally graded foams in the design of advanced adhesive materials. The combination of such energy absorbing materials and dry adhesives can open new avenues to produce dry elastic adhesives with high resistance to damage and de-bonding.

---

[1] *Footnote: this chapter is largely recreated from "Functionally graded dry adhesives based on film-terminated silicone foam"* [51] *published by the International Journal of Adhesion and Adhesives on February 4th 2017, copyright permission can be found below in "Letter(s) of Copyright Permission".*

Chapter 3. Multilayer Functionally Graded Material for Dry Adhesive Applications: Scaling from Micro to Macro Terminal Structures

Many fundamental theories on adhesion mechanics like contact geometry, contact splitting, and compliance has identified design parameters and defined a range of properties for adhesive engineers to create and better understand their adhesives. In this chapter, the universal application of soft backing material adhesion enhancement will be tested using mushroom capped structures in micro and millimetre scales.

Since the creation of soft lithography technique, many fast prototyping strategies and techniques have been developed for dry adhesive micro mould patterning. Silicon wafer direct peeling and etching [4] are common to transfer lithographic patterns to polymer materials. As 3D printing becomes more and more synonymous to being a matter replicator, the cost and feature resolution will eventually reach single micron accuracy. Even at current *tens* of micron resolutions, 3D printers have great advantages in cost of materials, ease of operation, efficient use of operator time, and allowance for high throughput operations. 3D printers do not need a large clean room, nor require harsh and highly toxic chemicals to fabricate moulds. Lastly, unlike traditional lithography, scaling features and printing is all completed via computer control, if the software aided digital designs are correctly made and sliced, printing is done with little to no supervision, drastically reducing human error and various chemical and particulate contaminants.

This study will evaluate the direct scaling of a micro mould by a ratio of 1:70, achieving the lowest printable limit of the 3D printer currently available at our facility. With the addition and integration of the fast sugar cube templating method, adhesive properties will be evaluated to determine if 3D printed moulds using the same design parameters of their micrometre cousins can be transferred quickly and easily without suffering a large penalty in performance. The polymer used for printing the mould is ABS and an acetone

vapour treatment step will be performed to smooth part roughness and to reflow material to fill gaps left by the printing process.

3.1. Materials and Methods

3.1.1. Fabrication of PDMS Samples

The fabrication steps are as summarized in the Figure 31. A mixture of PDMS (Sylgard 184, Dow Corning) at 10:1 weight ratio of polymer and curing agent were prepared, vortex mixed, and vacuum degassed for all samples. The PDMS control sample was cured in a small plastic petri dish. The film foam sample's terminal film was fabricated separately before fusing together with a PDMS soaked sugar cube.

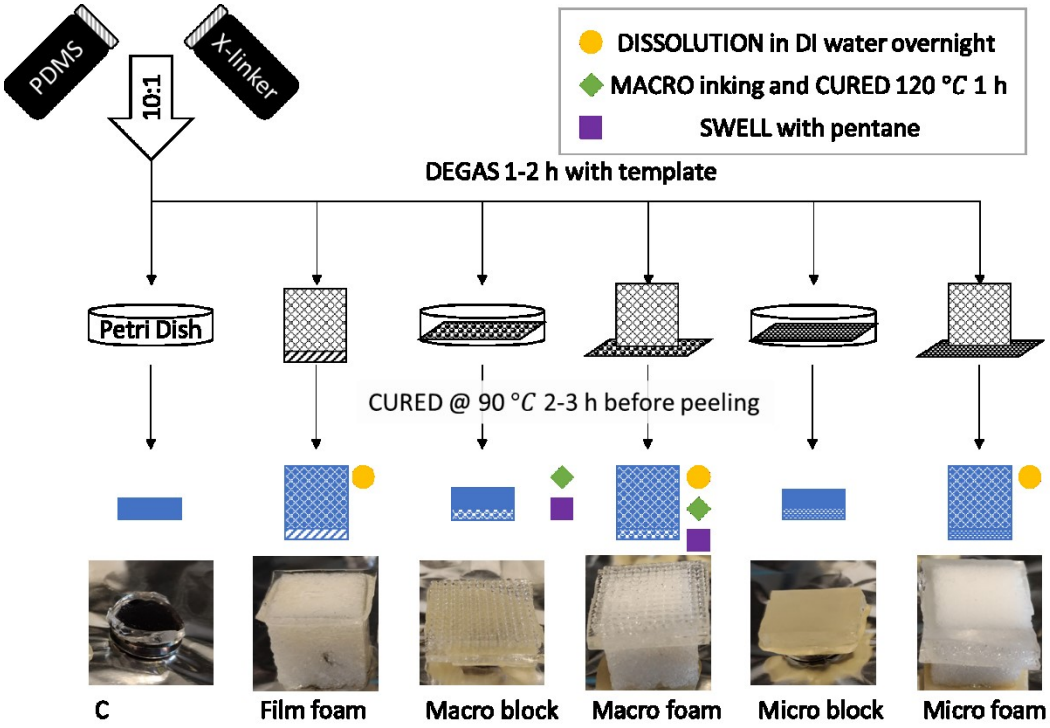

Figure 31: Summary of sample preparation

The terminal thin film was fabricated by pouring $2g$ of premixed PDMS onto a pre-treated flat <100> p-type silicon wafer (University Wafer) and spin-coated (Specialty Coating Systems G3-8) at $3500rpm$ for $45s$, rested for $5min$, and cured at $120°C$ for $1h$.

Sugar cube templates were placed into a petri dish of premixed PDMS and degassed for 1-$2h$ to displace the air within the template with polymer premix. Excess polymer was scrapped from the sides of

the polymer soaked sugar cubes using a plastic straight edge. The "foam film" sample saw the uncured cube was placed directly onto the cured film, which is still attached to the silicon wafer. All other foam moulded samples, the template was placed in a petri dish and degassed with the sugar cube sitting atop its respective mould.

The cube was left to rest for $5min$ with a small weight on its top face before being cured at $90°C$ for 2-3h. After cooling, the samples are detached from their respective moulds and any polymer flashing was trimmed. The dimensions of the sugar template were measured (n=20) to be: 15.63 ± 0.07 by 15.55 ± 0.09 by $15.56\pm0.14mm$, having a mass of $3.5261\pm0.0239g$.

All sugar template samples were placed into a container of DI water and left overnight to dissolve the template. PDMS samples were then oven dried at $120°C$ overnight to remove any moisture. Ethanol cleaning with KimWipe was completed between indentation tests. To avoid different sample treatments, all samples were left in the same DI water bath, dried in the oven together, and were otherwise treated to the same post curing steps. The resulting porosity of the PDMS foam is $70.62\pm1.78\%$.

Release Agent Coating

Silicon wafer and all moulds were pre-treatment with release agent to aid with unmoulding. FDTS (Gelest, Inc.) were added to a glass slide and moulds were suspended above the slide. The release agent was cured under vacuum at $90°C$ for $1h$. The flat silicon wafer was cleaned with ethanol and KimWipes and to remove any residue while the other moulds underwent PDMS moulding to remove residues.

Moulding and Mushroom Caps

The 3D printed ABS macro mould underwent acetone evaporative smoothing for $15min$ before being treated with previous release agent. The mould underwent PDMS moulding to create a PDMS master. The PDMS master itself was also treated with release agent before further replication.

The unmoulded PDMS pillars are dipped in a thin layer ($500rpm$ for 15-30s for 1-5min) of premixed PDMS as the inking step, left suspended for $5min$ before pressing onto a release agent treated glass slide and rested for $5min$ before curing. The assembly was cured at $120°C$ for $1h$ before leaving to

cool in room temperature. To detach the mushroom caps without damage, the assembly is dipped into pentane and the swelling detaches the pillars from the glass one by one, reducing the chance of damaging the mushroom caps.

The polyacrylate micro mould was provided by colleagues from the University of Alberta and Simon Fraser University, D. Sameoto and C. Menon [52]. The mould was created using deep UV patterning with built-in cap structures for moulding biomimetic dry adhesives.

To avoid differences in post treatment, all other samples were also swelled in pentane and dried together.

3.1.2. Characterization

Three controls were used during the investigation: a pristine block of PDMS, a micron sized mushroom caps on a PDMS block, and a millimetre sized mushroom caps on a PDMS block. They will be referred to as "C", "micro block", and "macro block".

The foam samples are as follows: a $19.10 \pm 0.37 \mu m$ film terminated PDMS foam pad, a micron sized mushroom caps on PDMS foam; and a millimetre sized mushroom caps on PDMS foam. They will be referred to as "film foam", "micro foam", and "macro foam".

Moulds

The moulded dimensions of the micro and macro mushroom caps are listed in Table 1. Imaging was completed via SEM for the micro mould and the macro mould was captured with a USB microscope camera (Dino-Lite Premier AD4113ZT). Measurements were completed using ImageJ (1.50i).

Table 1: Mould design dimensions and measurements

Mould	Material	Pillar Ø [µm]	Pillar length [µm]	Cap Ø [µm]	Spacing [µm]	Surface coverage [%]
Micro features (n = 10)	Polyacrylate theoretical	12	12	15	5	49.25 ±1.18
	PDMS sample	13.537 ±0.291	12.681 ±0.414	15.717 ±0.180	4.130 ±0.376	
Macro features (×70) (n = 10)	ABS theoretical	840	840	1050	350	61.97 ±6.80
	PDMS sample	884.896 ±51.683	1089.184 ±21.499	1218.924 ±75.870	153.272 ±98.028	

The macro features from the ×70 mould has longer than expected pillar length due to added material from the inking step to create the mushroom caps. The higher cap diameter with the associated smaller spacing is also due to the inking step; as the wet PDMS spreads while curing, it increases the cap diameter while decreasing the spacing, but the square centre-to-centre spacing is still maintained.

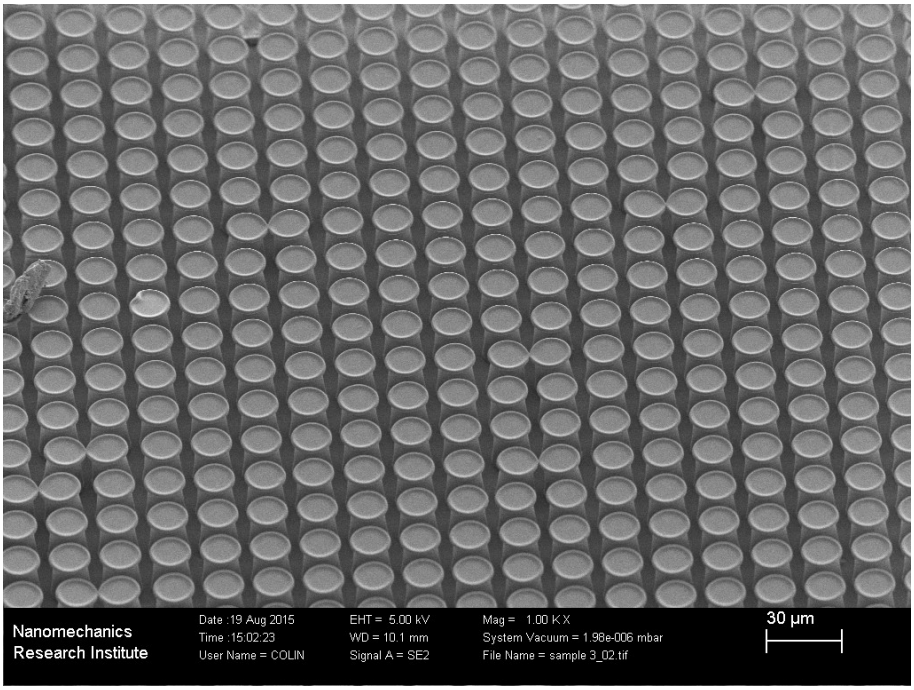

Figure 32: SEM showing the mushroom caps of PDMS micro block sample

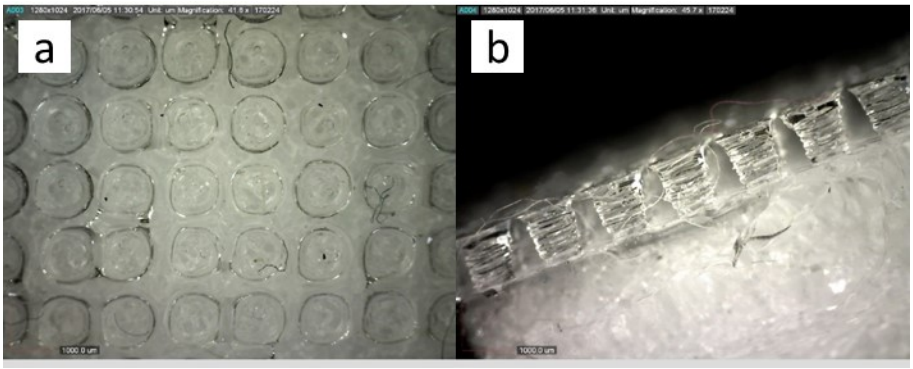

Figure 33: (a) Microscopy of mushroom caps; and (b) pillars of PDMS macro foam sample

A Fortus 360mc (FDM Technology) was used to print the macro mould at a part resolution of $\pm 0.0015 mm/mm$ (± 0.0015") to $\pm 0.127 mm$ (± 0.005") slice height using ABS at 100% fill. The original

model was designed using SolidWorks before slicing in Cura 2.3.0. The ABS mould was then casted in PDMS and the PDMS negative was used for sample making.

Due to the limitations of 3D printing, the pillar walls are not as straight as the micro pillars; however, the mushroom caps have higher priority and can be seen in Figure 32 and Figure 33 to be comparable to its micro cousin.

3.2. Results

Previously evaluating the adhesive behaviour of foam backed dry adhesives of the same material [51], found that controlling the softness of the adhesive pad in a geometrically graded fashion [5], resulted in modest increases in adhesive strength, work of adhesion, and energy dissipation. This report extends the investigation from flat featureless terminal ends to micro and macro mushroom terminal caps.

3.2.1. Force Displacement Curves

Figure 34 shows an example of a force-displacement curve. There are three main regions: the loading curve, the contact curve, and the pull-off curve. The preload force is determined as the peak force measured during the loading curve with the rate of approach of $10\mu m/s$. The set preloads are 100, 200, 300, 400, $500mN$ and 1, 2, 3, 4, $5N$ of force. The contact time is set for $1s$ for all tests. The pull-off force is determined as the peak force measured during the unloading curve with the rate of retraction of $10\mu m/s$. A 3" watch glass was used as the probe surface and was measured to be 2a= $76.85\pm0.50mm$ in diameter and h= $8.59\pm0.23mm$ in height. Using the spherical cap formula: $r = (a^2 + h^2)/2h$, the radius of curvature R= $90.28mm$ is calculated.

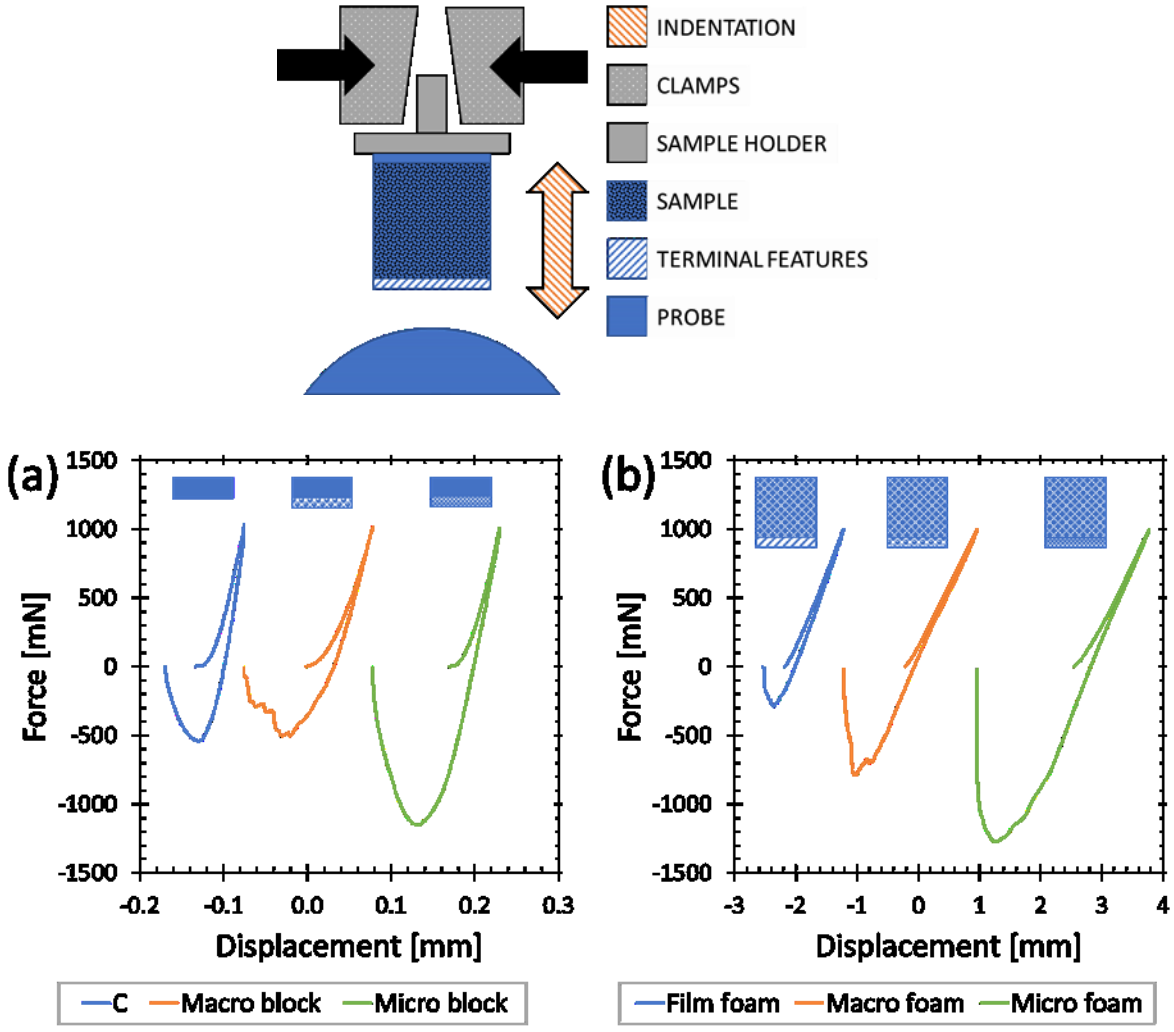

Figure 34: (top) UMT indentation setup; (bottom) 1N preload force displacement plot of (a) block and (b) foam samples

Figure 35 summarizes the preload and pull-off force curves with reported values arranged in Table 7 within the Appendices. The control sample "C", has the simplest geometry, a block of PDMS, thus has little preload dependence. Next, the "film foam" sample has some preload dependence, but overall performs worse than the control within this preload range. Comparing both mushroom capped samples "macro foam" and "micro foam", there is significant increases in pull-off force compared to their "macro block" and "micro block" counterparts. Providing some context, commercially available double-sided tape (3M poster tape) has a holding force of about $1/4lbs$ or $113g$ ($1.11N$).

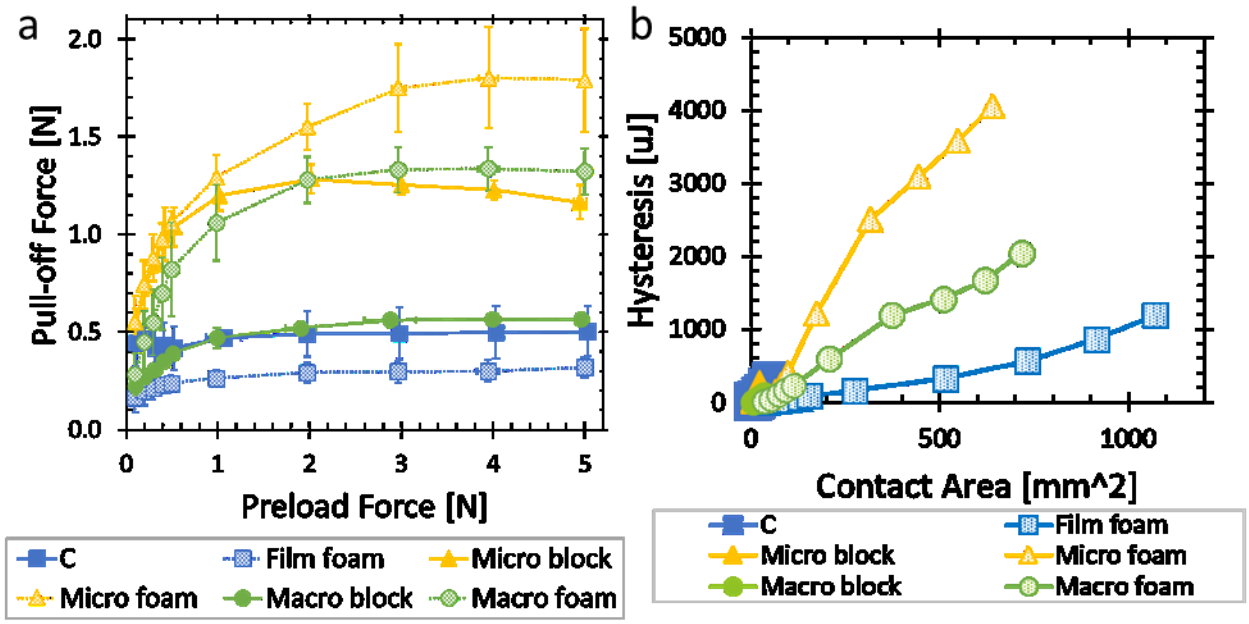

Figure 35: (a) Preload versus pull-off force of all block and foam samples; (b) calculated contact area work of adhesion plot

3.2.2. Displacement Hysteresis Curves

Due to characterization machine limitations, contact area could not be directly measured. Unfortunately, this means that the work of adhesion will be calculated estimates. Hysteresis is plotted by itself (real values) against the displacement of the probe into the sample in Figure 36. Herein, hysteresis is the energy difference between the loading and unloading curves. The displacement is simply the distance the probe has intruded into the sample.

There are *two* very distinct regions, the shorter displacement grouping representing the block backed dry adhesives, and the other for the foam backed samples. Foam backing has a significant effect in increasing the energy dissipation of such adhesive systems; the hysteresis is plotted in Figure 35.

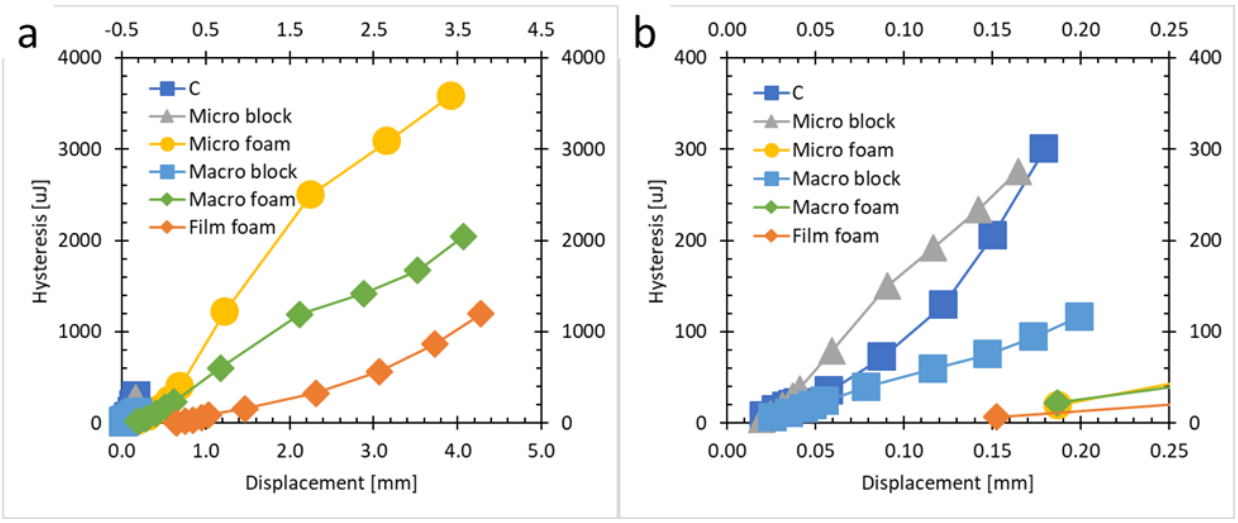

Figure 36: (a) Displacement hysteresis relationship of samples; (b) expanded region for block samples

3.2.3. Indentation Force Deflection (IFD)

Based on the D3574-11 Test B1 ASTM standard for "Flexible cellular materials – slab, bonded, and moulded urethane foams", the deflection force is reported for 25% and 65% IFD in Table 3. Modifications to the standard are as follows: flat metal plates larger in dimensions than the sample were used in place of perforated boards, sample size was limited by the sugar cube at approximately $(15mm)^3$, and a pre-flex deflection of 75% was selected. UMT load cell: DFH-100 ($100kg$).

Table 2: IFD values for PDMS foam

IFD (n = 8)	25% [mN]	STDEV	65% [mN]	STDEV
~70% porosity PDMS foam	510.27	72.54	5057.35	962.76

3.2.4. Scaling

Due to the high cost, fragility, and complexity of silicon micro patterned moulds, 3D printing was explored to ease the process of fast prototyping and mould making. The scaling from the micro to macro mould is approximately 1:70 and is at the limit of the 3D printer's capabilities. These millimetre features are interesting as seen in the recent work by Isla et al. [53] with their switchable release pillars. Our system in contrast can be detached through shear or torque, due to the foam backing material.

Even with an almost two magnitude change in scale, the compliant foam is still acting as an adhesion multiplier that increases the adhesive ability of surface features, such as the mushroom caps. At least within this range of 15 to 1050μm feature size, having a foam backing is a boon to increasing adhesive pull-off force. Following our simple fabrication steps using sugar cubes as the foam template, this might be a faster, more cost-efficient method of improving dry adhesives and seems to be applicable to micro to macro terminal structures.

Foam Pore Size Mismatch

The foam pore size and structure is the same for both the micro and macro samples as the sugar template was not scaled. Thus, the ratio of the pore size to terminal features is different for the micro vs macro moulds.

Non-standard Probe

Normally, it is standard practise to use either a flat punch or a 6mm hemispherical glass probe for indentation tests. However, flat punches result in alignment issues and 6mm diameter probes are far too small to fit even just one macro pillar within the view of microscope camera. Furthermore, the range of preload and pull-off forces far exceeds what is nominal for the load cell attached to the micro-indenter. Thus, it was determined to use a larger probe, a 3" watch glass to characterize the samples. This results in some discrepancies that were not considered in previous works. As such, it is difficult to resolve the lower pull-off force performance of the “film foam” sample compared to the control. Based on previous results, at low preload using the 6mm probe, the “film foam” configuration beats control. Thus, there might be a crossover point between probe curvature, preload, and foam samples that have not been captured. Future investigation with different probe curvatures might be necessary to determine if “film foam” and control block samples have a crossover point and if there is any effect on the micro and macro samples.

3.2.5. Application of PDMS Adhesive Pads

This foam backing material has the potential to universally improve adhesion tolerance, peel tolerance, moisture and cryogenic resistance, as well as being flexible enough to conform to surfaces. In Figure 37, a silicon wafer had the samples attached, was cooled in a -20°C freezer for 15min then removed

into ambient conditions. The surface was approximately -6°C in a 21°C room quickly condensed water vapour on its surface.

After peeling the adhesives to show that they are still working if attached prior to cooling, they are reattached in the presence of water and the tape fails to stay attached while all other samples can hold the combined weight of the wafer plus samples.

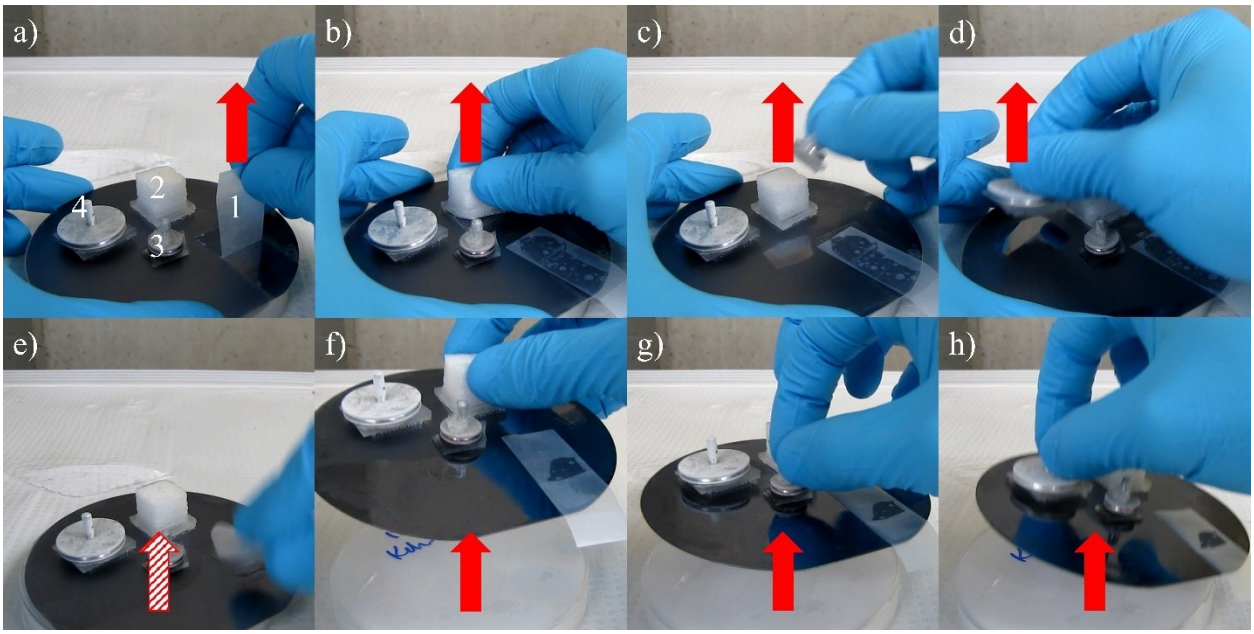

Figure 37: Still images from video of low temperature surface adhesion in ambient environment, a) peeling of tape, b) macro foam, c) control, and d) macro block sample. As well as the associated reattachment and lifting capabilities of e) tape, f) macro foam, g) control, and h) macro block.

The next demonstration shows the foam's vibration and peel tolerance. The samples are attached to glass slides perpendicular to a test arm that will push into it 5mm parallel to its adhered surface and 5mm perpendicular from its attachment point. Figure 38 shows the macro foam sample able to resist peeling and stays attached to the surface after a few seconds of deflection while the macro block sample immediately fails.

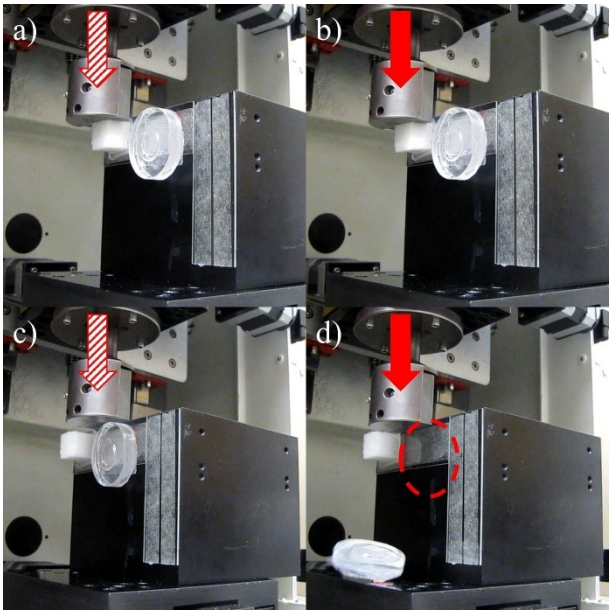

Figure 38: Still images from video of UMT knockoff test between a)-b) macro foam and c)-d) macro block. a) and c) showing contact of test arm with the sample and b) and d) the result of 5mm deflection into the sample's side.

3.3. Conclusions

It was determined, at least in the preload range of $100mN$ to $5N$, for micro to macro scale (1:70) of 15 to $1050\mu m$, the addition of foam backing material through sugar templating, increases pull-off strength by approximately 50% and 160% at high preload respectively. Due to the nature of foam materials, the hysteresis energy dissipation is also increased by several times compared to simple block backing. This innovative and simple improvement in the fabrication of dry adhesives allows the use of the same material avoiding material mismatch and can serve as a platform for all terminal structures be it micro or macro in scale. With this concept, future investigation of negative Poisson moulds and other controlled foam structures can be possible with advancements in 3D printed PDMS techniques. Other materials such as low viscosity PU have been successfully used to make polymer foams with the sugar templating process.

Chapter 4. Compression Study on Foam Porosity

The selection of a suitable sugar cube for the above studies were evaluated from various brands and types. The trade-off of using premade cubes to handmade variants were also investigated. Two sugar cube making processes were explored, 10% weight direct mixing of water with sugar granules and 95% humidity indirect water vapour fusing of loose sugar granules [20]. However, due to inconsistent quality in porosity (non-uniform and fragile) and shape (no flat faces), commercially produced sugar cubes were deemed the superior choice.

Available in local supermarkets across Ontario are *four* common sugar cubes marketed under *two* brands: Lantic Inc. and Redpath Sugar Ltd. as seen in Figure 39. Each brand has a white and raw sugar product; the samples are labelled by their manufacturer followed by a letter "W" to symbolize white sugar or "B" for raw brown sugar i.e. "LanticW" will be a sample of Lantic white sugar templated polymer cube.

Figure 39: Commercially purchased sugar cubes from Lantic Inc. and Redpath Sugar Ltd.

4.1. Porosity and Pull-off Dependence

The porosity of each sample was first determined, followed by a compressive test. Pull-off force data was collected at the end.

4.1.1. Porosity

As can be seen in Table 3, raw sugar cubes, in general, have higher polymer porosity due to their dense packing. However, they are slightly smaller in *two* of its dimensions, thus reducing the overall volume and size of the adhesive pad. Since the last dimension is similar to the other cube thicknesses, the terminal film was attached to one of the two faces that share that depth.

Table 3: Summary of porosity and volume measurements of sugar templated polymer cubes

Brand	Type	PDMS Porosity [%]	Volume [mm^3]	Thickness [mm]
Lantic	White (n=12)	70.06±1.49	3729.04±24.96	15.53±0.20
	Raw (n=12)	72.84±0.71	3429.33±52.49	15.12±0.13
Redpath	White (n=12)	68.96±0.86	3753.62±42.65	15.39±0.08
	Raw (n=4)	72.07±0.26	3440.79±10.63	15.16±0.02

4.1.2. Indentation Force Deflection

In terms of foams, we expect greater porosity to result in a softer material. As such, IFD as defined in section 3.2.3 was completed for the sugar cubes to determine their stiffness. As seen in Table 4, raw sugar cubes with higher porosity has significantly lower stiffness in both the low and high compression tests compared to their white sugar counterparts. Although the high porosity low stiffness sample would have been the ideal sample, it was quickly discovered that the thinner polymer cell walls of the foam air cavity is unable to withstand its own adhesive force. At higher preloads with higher pull-off forces, terminal film detachment from the foam layer is observed. This is detrimental to its reusability.

Table 4: Summary of IFD stiffness measurements of sugar templated polymer cubes

Deflection [mN]	Lantic		Redpath	
	White (n= 8)	Raw (n=8)	White (n=8)	Raw (n=4)
IFD25%	510.27±72.54	270.32±81.44	437.36±112.67	282.22±53.12
IFD65%	5057.35±962.76	1635.26±324.04	4121.20±960.39	3277.71±320.78

Figure 40 shows the deflection curve and sample measured force of the IFD test. At constant speed, the samples experience *two* pre-flex indentations at 75% of the thickness of the sample in the first 15*s*,

followed by a 360*s* relaxation period before the 25% of 65% IFD, the value is read at the end of a 60*s* holding period.

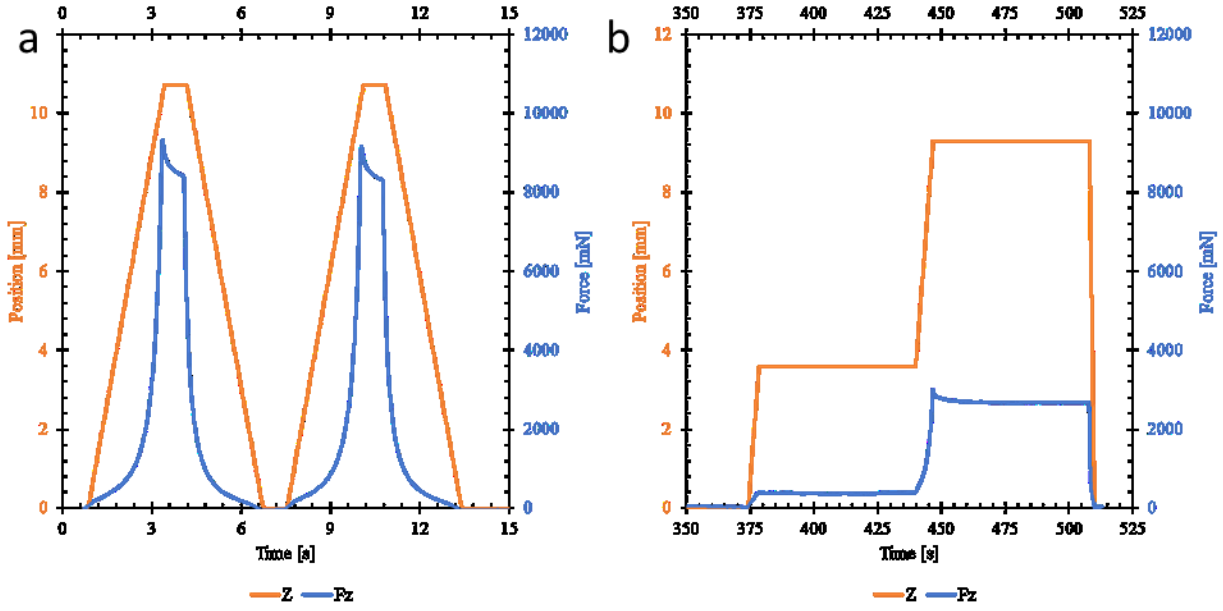

Figure 40: Sample IFD force displacement curve of Lantic raw sugar templated polymer cube: (a) is the first 15s and (b) last 125s of the test displacement and resulting deflection force

The resulting IFD forces with sample foam porosities are presented in Figure 41. In general, higher polymer porosity results in lower material stiffness. A change in sugar porosity of approximately 4% can produce a difference in stiffness of 200-300%. Due to the limitation of commercially available sugar cubes, other porosities were not investigated.

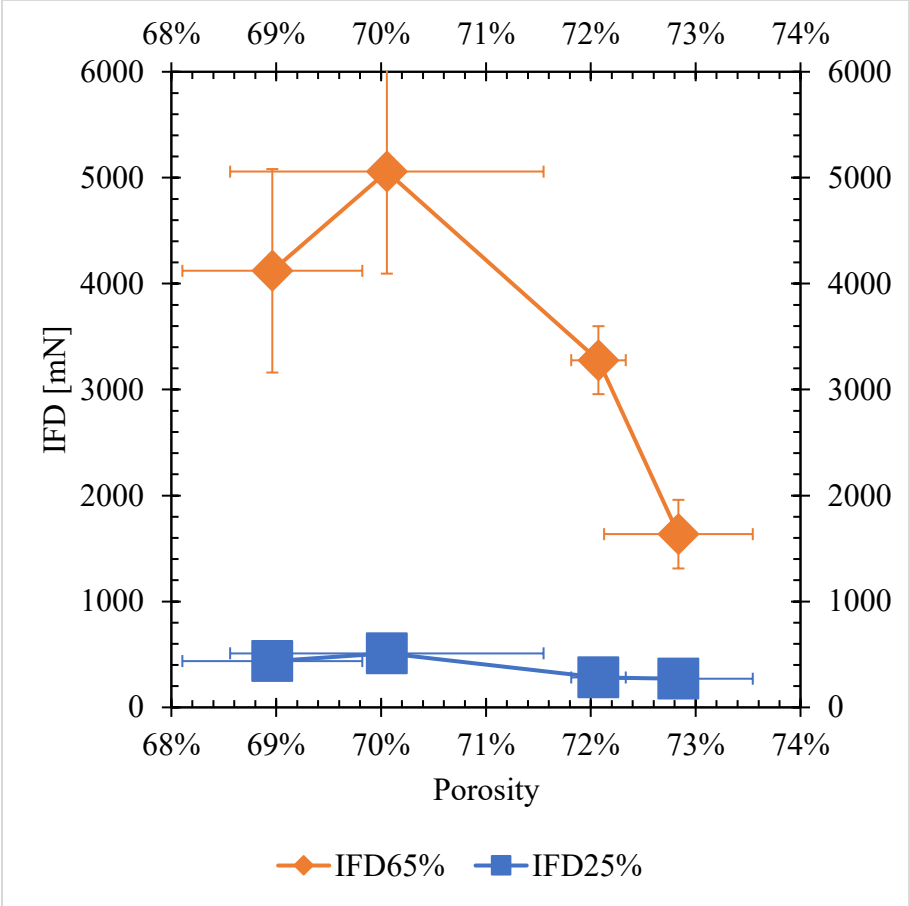

Figure 41: Relationship of foam porosity and IFD stiffness

4.2. Pull-off Relationship

Pull-off tests were performed using the $6mm$ glass hemispherical setup described in 2.1.2. The pull-off data for the *four* sugar samples were fitted to a non-orthogonal *three* factor (*two* 2-level, *one* 8-level) linear model. After *three* iterations, the reduced model is: $y = B_0 + B_1 * preload + B_3 * type$; where the preload is the force applied in millinewtons (mN) and type equals -1 for white sugar and 1 for raw sugar. The ANOVA analysis is available in Table 5 and the parameter values in Table 6. The analysis roughly estimates parameter coefficients assuming linearity. Only the type of sugar and preload force was determined to have a significant effect on pull-off force. From this analysis, higher preloads and white sugar templates optimises the pull-off force.

Table 5: ANOVA table for reduced model, evaluating brand, sugar type, and preload dependence

ANOVA					
Source	SS	df	MS	F	
Regression	95.59	2	47.80	88.27	Probe
Error	135.36	250	0.54	3.86	$F_{0.01,3,250}$
Total	230.95	252		2.60	$t_{0.01/2,250}$
s^2	0.54				

Table 6: Parameter values for reduced model indicating only preload and sugar type significance

Parameter	Coefficients	$\pm$	Description
B_0	2.3298	0.1369	Intercept
B_1	0.0236	0.0055	Preload
B_3	-0.3511	0.1248	Sugar type

The pull-off plots: Figure 42 and Figure 43 show "Redpath W" sugar templated samples to have the best performance. All foam samples at all preloads (in this range) perform better than the control polymer block.

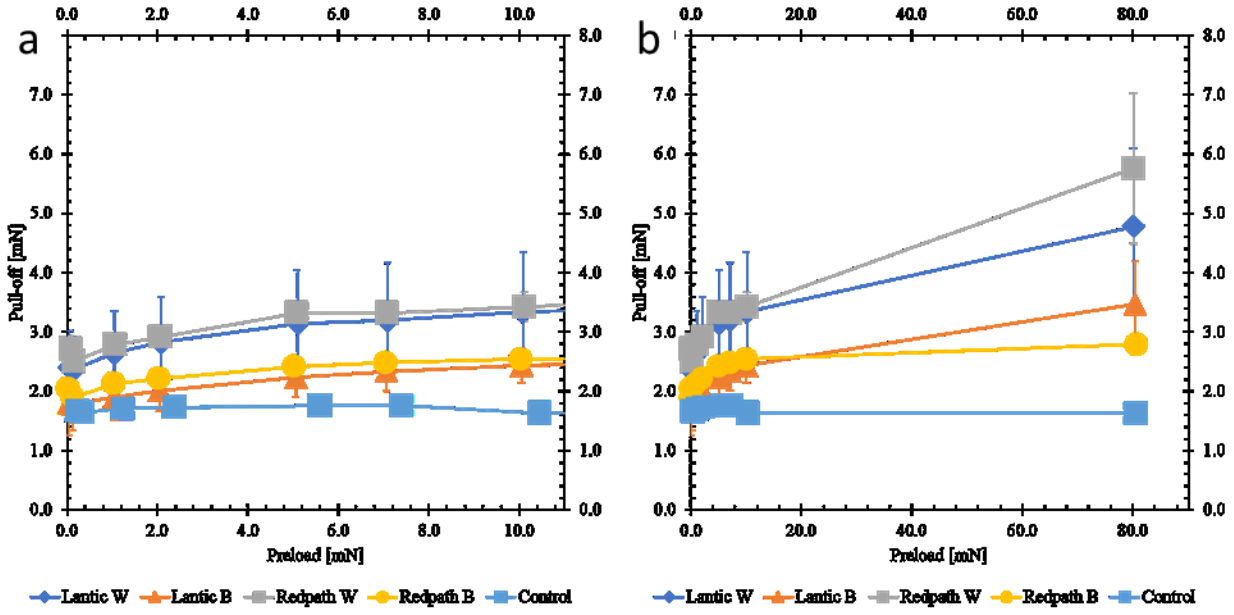

Figure 42: Preload and pull-off relationship of samples at (a) low and, (b) full preload range

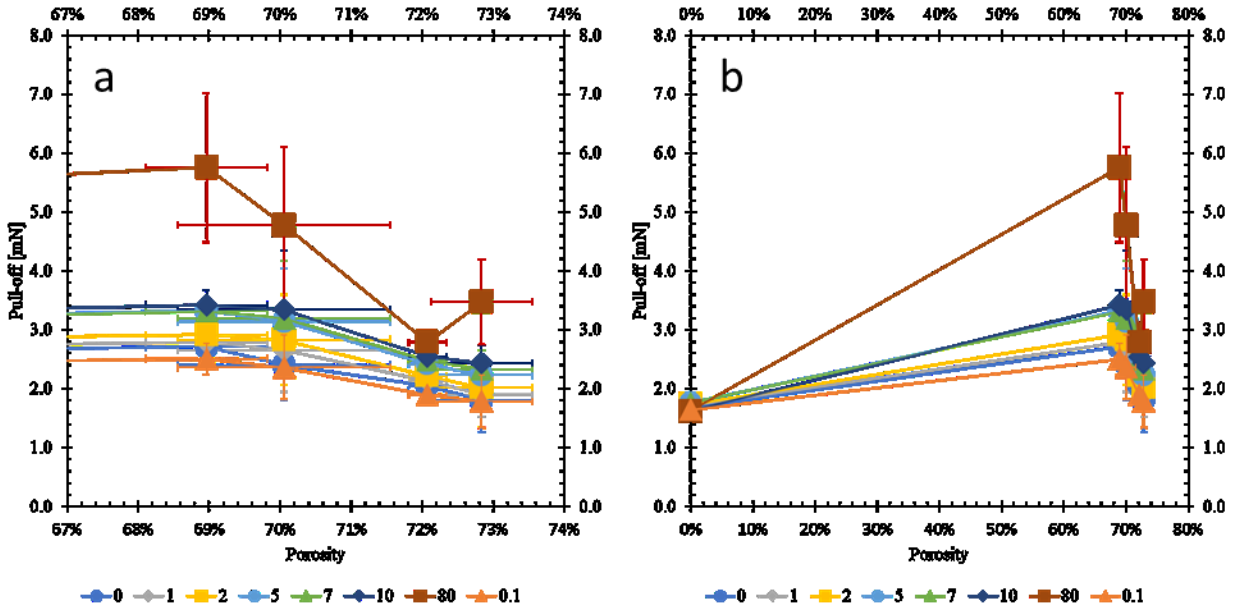

Figure 43: Porosity and pull-off relationship of samples at different preloads (mN) for (a) porous samples only and, (b) including the control sample

4.3. Conclusion

It was determined that small changes in porosity produces large changes in foam stiffness. Higher polymer porosity results in lower stiffness with the trade-off of thinner foam cell walls. Using simple non-orthogonal linear modelling, sugar brand and all multi-factor interacts were found to be insignificant. Sugar type and preload forces were the only significant terms in determining pull-off force. Overall, white sugar templates obtained the highest pull-off forces when compared to the other samples, while all foam samples resulted in higher results than the control sample in the range of 0-80mN preload using the 6mm hemispherical probe. Thus, commercially produced white sugar templates made from "RedpathW" and "LanticW" polymer cubes were used in all future studies.

Chapter 5. Concluding Remarks and Recommendations

Unlike a simple polymer block, the attachment of a soft backing material to terminal dry adhesive structures can improve adhesive strength, as measured by pull-off force and work of adhesion. The work presented in this thesis indicates that the backing material is an important adhesive design parameter currently less explored. The range of improvements in adhesion characteristics seen previously with the addition of a soft backing material to a film terminated structure, are generalizable to other terminal structures as micro and macro mushroom capped structures were successfully fabricated. Lastly, the porosity and thickness of the backing materials has been optimized for the sugar cube, using statistical modelling that shows the significant contribution of sugar cube type and preload to pull-off force.

Using a granular sacrificial template has the advantage of fast prototyping, and its integration with 3D printed moulds helps accelerate the development and understanding of adhesive pad design. The simple fabrication of polymer foam using sugar linked with the standard soft lithography methods of pattern transfer, is a highly modular design approach. The adhesive pads are assembled by selecting interchangeable components for terminal end structures and backing geometry combinations, thereby providing the designer with ease of fabrication and replication. Further, as the master moulds are not damaged, they need only be designed and made once. The sugar template method also has the advantage of using only one material for the composition of the adhesive pad, avoiding material incompatibility while improving polymer cohesion.

The studies presented herein have also collected and integrated foam stiffness with indentation studies, identifying the standardized testing parameters and reporting material property values for future comparative study and reference. Finally, some end applications of the product have been demonstrated: a robotic pick and place arm, adhesion in high moisture and low temperature environments, and the adhesive pad's tolerance to lateral deflection. In conclusion, the thesis objective is complete as the foam thickness, various terminal structures, and porosity/stiffness PDMS foam were tried and tested.

Based on the findings of the studies completed herein, to optimize an adhesive pad design for dry adhesives, a mushroom structure decorated atop pillars which in turn sits above a soft porous material of the same material is ideal. The contact splitting of the terminal structures into smaller regions (the smaller the greater the adhesion), although it decreases the overall contact area, has significant benefits in creating crack trapping locations and impedes crack front propagation. Having pillar support struts help to impart some compliance and independent flexibility and energy absorption for each mushroom cap, akin to that of a shock absorbing compression spring. Lastly, the porous backing material (white sugar cubes of 10-15mm thickness of approximately 70% porosity) provides even more energy dissipation and further flexibility to conform to curved surfaces while restricting unwanted deflection forces, thus allowing smart control of adhesive release in the form of controlled shearing or torque. Further, as shown in our 70 time scale up of the micro mould, the foam backing material is effective for direct application to features spanning from micron to millimetre scales, thus there should be no terminal structure restrictions. The sugar cube studies have shown that only the preload and sugar type (porosity) played a significant role in contributing to pull-off force, as evaluated via statistical analysis and modelling. In this sense, any brand of sugar cube can be used so long as it has flat surfaces for terminal structure attachment.

The backing material properties of dry adhesives is an important parameter and should be considered when designing dry adhesive systems as they provide greatly improved pull-off force and work of adhesion characteristics compared to simple non-porous backing substrates of the same material.

5.1. Future Work

At the end of this thesis, some potential topics of study have been identified for future investigation. In the above studies, commercially produced sugar cubes were used instead of in house made sugar templates due to inconsistencies in the sugar fusing process of handmade samples. However, there is no way of controlling the parameters of commercially purchased sugar cubes which results in little control of the sugar granule distribution and thus the geometry of the polymer copy. The printing of silicon materials and PDMS is rising in popularity as demonstrated by Structur3D Printing a local 3D solutions company who sells a silicon injector attachment for commercial 3D printers. With the advent of this technology, porous backing material can be extruded layer-by-layer, controlling substrate parameters such as cell wall thickness, porosity, Poisson ratio, cavity dimensions and shape, and eases scalability.

On that vain, it would be extensively interesting to investigate negative Poisson ratio geometries and their impact on adhesion properties by selecting origami geometric designs for both the terminal end structures and supporting backing material such as the Miura-*ori* (fold), herringbone tessellation, hilula and cube tessellation, triangle and hexagon twist just to name a few. Other auxetic patterns outside of origami includes the bowtie and fractal pattern.

Lastly, there is value in investigating the effect of probe radius of curvature on the pull-off force as in this thesis, *two* probes of different radii of curvature was investigated and the results hint at probe curvature dependence for some terminal geometries.

Letter(s) of Copyright Permission

NATURE PUBLISHING GROUP LICENSE TERMS AND CONDITIONS

Jun 27, 2017

This Agreement between University of Waterloo -- Kelvin Liew ("You") and Nature Publishing Group ("Nature Publishing Group") consists of your license details and the terms and conditions provided by Nature Publishing Group and Copyright Clearance Center.

License Number	4137121040612
License date	Jun 27, 2017
Licensed Content Publisher	Nature Publishing Group
Licensed Content Publication	Nature
Licensed Content Title	Adhesive force of a single gecko foot-hair
Licensed Content Author	Kellar Autumn, Yiching A. Liang, S. Tonia Hsieh, Wolfgang Zesch, Wai Pang Chan et al.
Licensed Content Date	Jun 8, 2000
Licensed Content Volume	405
Licensed Content Issue	6787
Type of Use	reuse in a dissertation / thesis
Requestor type	academic/educational
Format	print and electronic
Portion	figures/tables/illustrations
Number of figures/tables/illustrations	2
Figures	Figure 1 Figure 2
Author of this NPG article	no
Your reference number	
Title of your thesis / dissertation	Improving the adhesive properties and fabrication of multilayer biomimetic dry adhesives through the introduction and control of a foam based backing material achieved through sugar cube template moulding technique
Expected completion date	Jul 2017
Estimated size (number of pages)	100
Requestor Location	University of Waterloo 200 University Ave W Waterloo, ON N2L3G1 Canada Attn: University of Waterloo
Billing Type	Invoice
Billing Address	University of Waterloo 200 University Ave W Waterloo, ON N2L3G1

For Autumn et al. Figure 1 and Figure 2 [1] copyright permissions

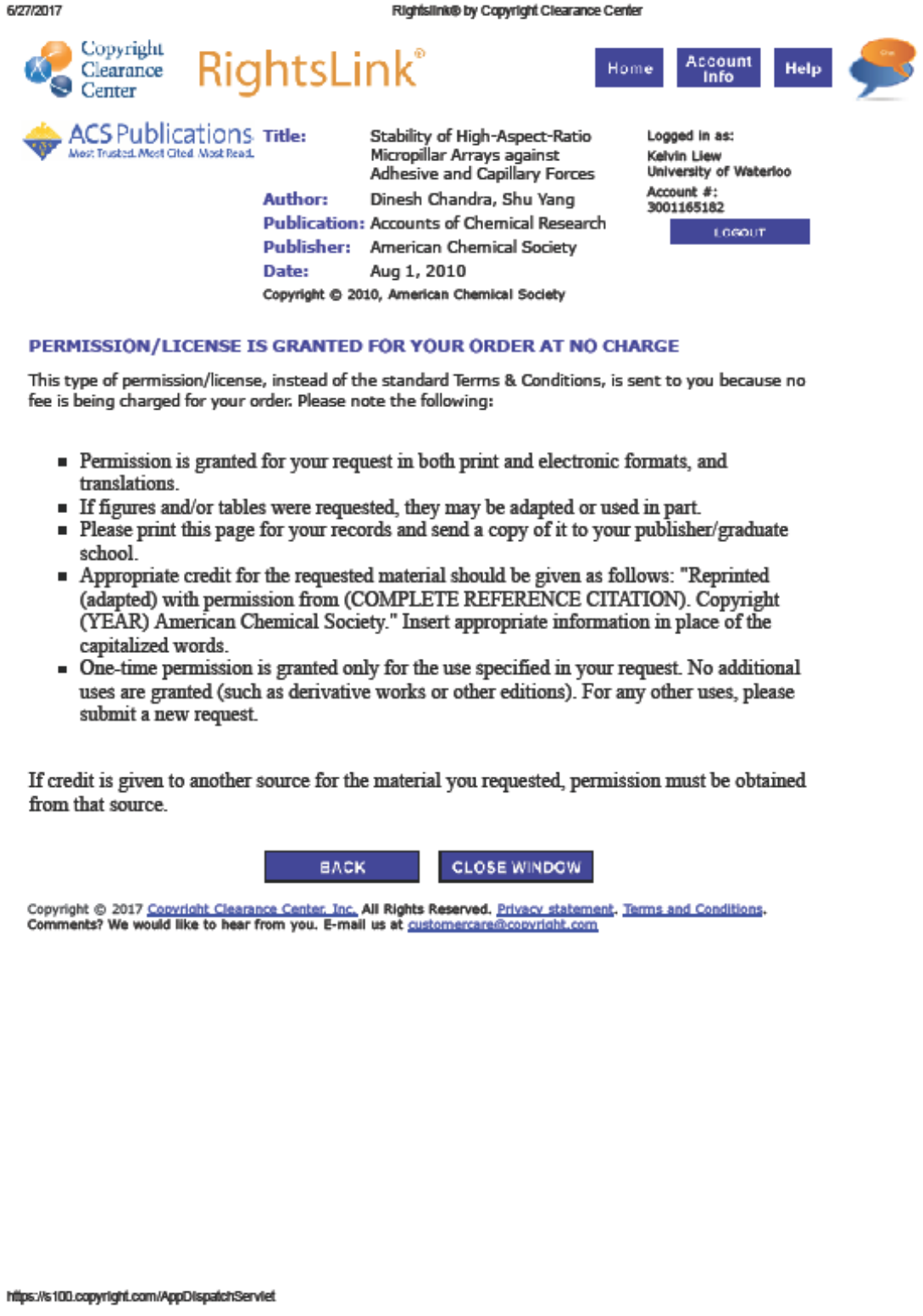

For Chandra et al. Figure 3 [6] copyright permissions

ROYAL SOCIETY OF CHEMISTRY LICENSE TERMS AND CONDITIONS

Jul 03, 2017

This Agreement between University of Waterloo -- Kelvin Liew ("You") and Royal Society of Chemistry ("Royal Society of Chemistry") consists of your license details and the terms and conditions provided by Royal Society of Chemistry and Copyright Clearance Center.

License Number	4141450022652
License date	Jul 03, 2017
Licensed Content Publisher	Royal Society of Chemistry
Licensed Content Publication	Soft Matter
Licensed Content Title	Biologically inspired enhancement of pressure-sensitive adhesives using a thin film-terminated fibrillar interface
Licensed Content Author	Hamed Shahsavan,Boxin Zhao
Licensed Content Date	Jun 14, 2012
Licensed Content Volume	8
Licensed Content Issue	32
Type of Use	Thesis/Dissertation
Requestor type	academic/educational
Portion	figures/tables/images
Number of figures/tables/images	1
Format	print and electronic
Distribution quantity	10
Will you be translating?	no
Order reference number	
Title of the thesis/dissertation	Improving the adhesive properties and fabrication of multilayer biomimetic dry adhesives through the introduction and control of a foam based backing material achieved through sugar cube template moulding technique
Expected completion date	Jul 2017
Estimated size	100
Requestor Location	University of Waterloo 200 University Ave W Waterloo, ON N2L3G1 Canada Attn: University of Waterloo
Billing Type	Invoice
Billing Address	University of Waterloo 200 University Ave W Waterloo, ON N2L3G1

For Shahsavan et al. Figure 4 [7] copyright permissions

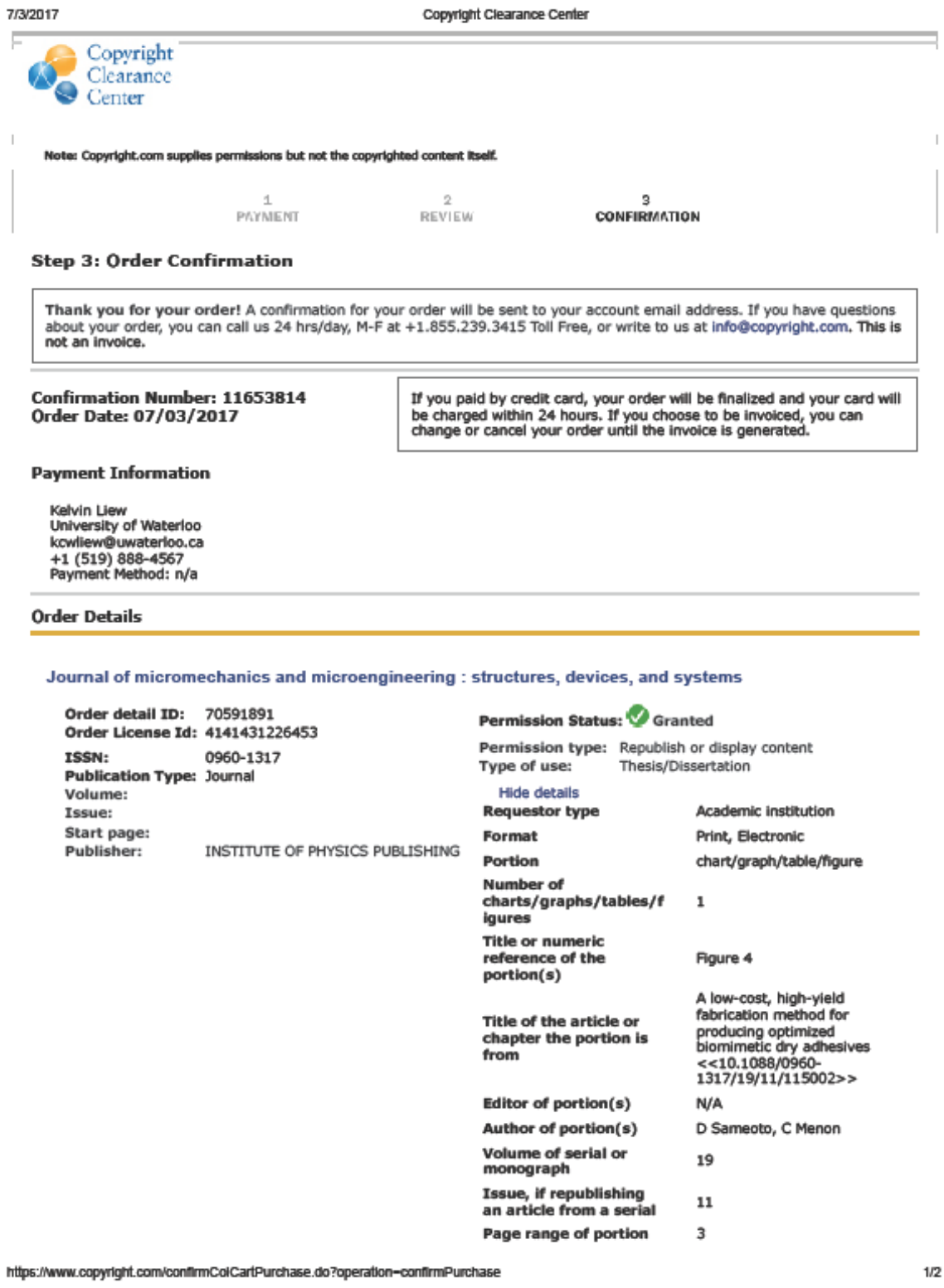

7/3/2017 Copyright Clearance Center

Copyright Clearance Center

Note: Copyright.com supplies permissions but not the copyrighted content itself.

1 PAYMENT 2 REVIEW 3 CONFIRMATION

Step 3: Order Confirmation

Thank you for your order! A confirmation for your order will be sent to your account email address. If you have questions about your order, you can call us 24 hrs/day, M-F at +1.855.239.3415 Toll Free, or write to us at info@copyright.com. **This is not an invoice.**

Confirmation Number: 11653814
Order Date: 07/03/2017

If you paid by credit card, your order will be finalized and your card will be charged within 24 hours. If you choose to be invoiced, you can change or cancel your order until the invoice is generated.

Payment Information

Kelvin Liew
University of Waterloo
kcwliew@uwaterloo.ca
+1 (519) 888-4567
Payment Method: n/a

Order Details

Journal of micromechanics and microengineering : structures, devices, and systems

Order detail ID:	70591891
Order License Id:	4141431226453
ISSN:	0960-1317
Publication Type:	Journal
Volume:	
Issue:	
Start page:	
Publisher:	INSTITUTE OF PHYSICS PUBLISHING

Permission Status: Granted

Permission type: Republish or display content
Type of use: Thesis/Dissertation

Hide details

Requestor type	Academic institution
Format	Print, Electronic
Portion	chart/graph/table/figure
Number of charts/graphs/tables/figures	1
Title or numeric reference of the portion(s)	Figure 4
Title of the article or chapter the portion is from	A low-cost, high-yield fabrication method for producing optimized biomimetic dry adhesives <<10.1088/0960-1317/19/11/115002>>
Editor of portion(s)	N/A
Author of portion(s)	D Sameoto, C Menon
Volume of serial or monograph	19
Issue, if republishing an article from a serial	11
Page range of portion	3

https://www.copyright.com/confirmColCartPurchase.do?operation=confirmPurchase 1/2

For Sameoto et al. Figure 5 [8] copyright permissions

JOHN WILEY AND SONS LICENSE TERMS AND CONDITIONS

Jul 03, 2017

This Agreement between University of Waterloo -- Kelvin Liew ("You") and John Wiley and Sons ("John Wiley and Sons") consists of your license details and the terms and conditions provided by John Wiley and Sons and Copyright Clearance Center.

License Number	4141440797151
License date	Jul 03, 2017
Licensed Content Publisher	John Wiley and Sons
Licensed Content Publication	Small
Licensed Content Title	Gecko-Inspired Directional and Controllable Adhesion
Licensed Content Author	Michael P. Murphy,Burak Aksak,Metin Sitti
Licensed Content Date	Dec 29, 2008
Licensed Content Pages	6
Type of use	Dissertation/Thesis
Requestor type	University/Academic
Format	Print and electronic
Portion	Figure/table
Number of figures/tables	1
Original Wiley figure/table number(s)	Figure 1
Will you be translating?	No
Title of your thesis / dissertation	Improving the adhesive properties and fabrication of multilayer biomimetic dry adhesives through the introduction and control of a foam based backing material achieved through sugar cube template moulding technique
Expected completion date	Jul 2017
Expected size (number of pages)	100
Requestor Location	University of Waterloo 200 University Ave W Waterloo, ON N2L3G1 Canada Attn: University of Waterloo
Publisher Tax ID	EU826007151
Billing Type	Invoice
Billing Address	University of Waterloo 200 University Ave W Waterloo, ON N2L3G1 Canada Attn: University of Waterloo

For Murphy et al. Figure 6 [9] copyright permissions

RightsLink®

Home | Account Info | Help

Title: Enhanced Adhesion by Gecko-Inspired Hierarchical Fibrillar Adhesives

Author: Michael P. Murphy, Seok Kim, Metin Sitti

Publication: Applied Materials

Publisher: American Chemical Society

Date: Apr 1, 2009

Logged in as:
Kelvin Liew
University of Waterloo
Account #:
3001165182

LOGOUT

PERMISSION/LICENSE IS GRANTED FOR YOUR ORDER AT NO CHARGE

This type of permission/license, instead of the standard Terms & Conditions, is sent to you because no fee is being charged for your order. Please note the following:

- Permission is granted for your request in both print and electronic formats, and translations.
- If figures and/or tables were requested, they may be adapted or used in part.
- Please print this page for your records and send a copy of it to your publisher/graduate school.
- Appropriate credit for the requested material should be given as follows: "Reprinted (adapted) with permission from (COMPLETE REFERENCE CITATION). Copyright (YEAR) American Chemical Society." Insert appropriate information in place of the capitalized words.
- One-time permission is granted only for the use specified in your request. No additional uses are granted (such as derivative works or other editions). For any other uses, please submit a new request.

If credit is given to another source for the material you requested, permission must be obtained from that source.

BACK | CLOSE WINDOW

For Murphy et al. Figure 7 [10] copyright permissions

7/3/2017 RightsLink® by Copyright Clearance Center

Copyright Clearance Center RightsLink®

Home | Account Info | Help

ACS Publications Most Trusted. Most Cited. Most Read.

Title: Bioinspired Functionally Graded Adhesive Materials: Synergetic Interplay of Top Viscous–Elastic Layers with Base Micropillars

Author: Hamed Shahsavan, Boxin Zhao

Publication: Macromolecules

Publisher: American Chemical Society

Date: Jan 1, 2014

Copyright © 2014, American Chemical Society

Logged in as:
Kelvin Liew
University of Waterloo
Account #:
3001165182

LOGOUT

PERMISSION/LICENSE IS GRANTED FOR YOUR ORDER AT NO CHARGE

This type of permission/license, instead of the standard Terms & Conditions, is sent to you because no fee is being charged for your order. Please note the following:

- Permission is granted for your request in both print and electronic formats, and translations.
- If figures and/or tables were requested, they may be adapted or used in part.
- Please print this page for your records and send a copy of it to your publisher/graduate school.
- Appropriate credit for the requested material should be given as follows: "Reprinted (adapted) with permission from (COMPLETE REFERENCE CITATION). Copyright (YEAR) American Chemical Society." Insert appropriate information in place of the capitalized words.
- One-time permission is granted only for the use specified in your request. No additional uses are granted (such as derivative works or other editions). For any other uses, please submit a new request.

If credit is given to another source for the material you requested, permission must be obtained from that source.

BACK CLOSE WINDOW

Copyright © 2017 Copyright Clearance Center, Inc. All Rights Reserved. Privacy statement. Terms and Conditions.
Comments? We would like to hear from you. E-mail us at customercare@copyright.com

https://s100.copyright.com/AppDispatchServlet 1/1

For Shahsavan et al. Figure 8 [5] copyright permissions

Creative Commons License Deed

Attribution-ShareAlike 3.0 Unported (CC BY-SA 3.0)

This is a human-readable summary of (and not a substitute for) the license.

You are free to:

Share — copy and redistribute the material in any medium or format

Adapt — remix, transform, and build upon the material

for any purpose, even commercially.

The licensor cannot revoke these freedoms as long as you follow the license terms.

Under the following terms:

Attribution — You must give appropriate credit, provide a link to the license, and indicate if changes were made. You may do so in any reasonable manner, but not in any way that suggests the licensor endorses you or your use.

ShareAlike — If you remix, transform, or build upon the material, you must distribute your contributions under the same license as the original.

No additional restrictions — You may not apply legal terms or technological measures that legally restrict others from doing anything the license permits.

Notices:

You do not have to comply with the license for elements of the material in the public domain or where your use is permitted by an applicable exception or limitation.

No warranties are given. The license may not give you all of the permissions necessary for your intended use. For example, other rights such as publicity, privacy, or moral rights may limit how you use the material.

For Wikipedia Figure 9 and Figure 10 copyright permissions

JOHN WILEY AND SONS LICENSE TERMS AND CONDITIONS

Jun 23, 2017

This Agreement between University of Waterloo -- Kelvin Liew ("You") and John Wiley and Sons ("John Wiley and Sons") consists of your license details and the terms and conditions provided by John Wiley and Sons and Copyright Clearance Center.

License Number	4134851369181
License date	Jun 23, 2017
Licensed Content Publisher	John Wiley and Sons
Licensed Content Publication	Journal of Biomedical Materials Research
Licensed Content Title	Fabrication of porous biodegradable polymer scaffolds using a solvent merging/particulate leaching method
Licensed Content Author	Chun-Jen Liao,Chin-Fu Chen,Jui-Hsiang Chen,Shu-Fung Chiang,Yu-Ju Lin,Ken-Yuan Chang
Licensed Content Date	Dec 12, 2001
Licensed Content Pages	6
Type of use	Dissertation/Thesis
Requestor type	University/Academic
Format	Print and electronic
Portion	Figure/table
Number of figures/tables	3
Original Wiley figure/table number(s)	Figure 1 Figure 3 Figure 4
Will you be translating?	No
Title of your thesis / dissertation	Improving the adhesive properties and fabrication of multilayer biomimetic dry adhesives through the introduction and control of a foam based backing material achieved through sugar cube template moulding technique
Expected completion date	Jul 2017
Expected size (number of pages)	100
Requestor Location	University of Waterloo 200 University Ave W Waterloo, ON N2L3G1 Canada Attn: University of Waterloo
Publisher Tax ID	EU826007151
Billing Type	Invoice
Billing Address	University of Waterloo 200 University Ave W Waterloo, ON N2L3G1

For Liao et al. Figure 11 [18] copyright permissions

JOHN WILEY AND SONS LICENSE TERMS AND CONDITIONS

Jun 23, 2017

This Agreement between University of Waterloo -- Kelvin Liew ("You") and John Wiley and Sons ("John Wiley and Sons") consists of your license details and the terms and conditions provided by John Wiley and Sons and Copyright Clearance Center.

License Number	4134881107448
License date	Jun 23, 2017
Licensed Content Publisher	John Wiley and Sons
Licensed Content Publication	Macromolecular Chemistry and Physics
Licensed Content Title	A Simple Water-Based Synthesis of Au Nanoparticle/PDMS Composites for Water Purification and Targeted Drug Release
Licensed Content Author	Adina Scott,Ritu Gupta,Giridhar U. Kulkarni
Licensed Content Date	Jun 9, 2010
Licensed Content Pages	8
Type of use	Dissertation/Thesis
Requestor type	University/Academic
Format	Print and electronic
Portion	Figure/table
Number of figures/tables	2
Original Wiley figure/table number(s)	Figure 1 Figure 2
Will you be translating?	No
Title of your thesis / dissertation	Improving the adhesive properties and fabrication of multilayer biomimetic dry adhesives through the introduction and control of a foam based backing material achieved through sugar cube template moulding technique
Expected completion date	Jul 2017
Expected size (number of pages)	100
Requestor Location	University of Waterloo 200 University Ave W Waterloo, ON N2L3G1 Canada Attn: University of Waterloo
Publisher Tax ID	EU826007151
Billing Type	Invoice
Billing Address	University of Waterloo 200 University Ave W Waterloo, ON N2L3G1 Canada Attn: University of Waterloo

For Scott et al. Figure 12 [19] copyright permissions

Gmail Kelvin Liew <kcwliew92@gmail.com>

re: thesis reuse of article

2 messages

Kelvin Liew <kcwliew@uwaterloo.ca> Fri, Jun 23, 2017 at 1:37 PM
To: reprints@liebertpub.com

To whom this may concern,

I would like to reuse Figure 1, 2, 3, and 5 of this article for my thesis: http://online.liebertpub.com/doi/abs/10.1089/107632702753503045

Following the instructions, there is no option for thesis, thus the email.

Please advise on options.

–
Regards,

Kelvin Liew | 20370088 | Candidate for MASc Chemical Engineering (Nanotechnology)
University of Waterloo | Surface Science and Bio-nanomaterials Laboratory
519.888.4567 ext.31671 | UW-CEGSA Health and Safety Rep.

Ballen, Karen <KBallen@liebertpub.com> Fri, Jun 23, 2017 at 2:14 PM
To: Kelvin Liew <kcwliew@uwaterloo.ca>

Dear Kelvin:

Copyright permission is granted for use of the figures requested for your thesis.

Kind regards,

Karen Ballen

Manager, Reprints, Permissions and Open Access

From: kcwliew92@gmail.com [mailto:kcwliew92@gmail.com] **On Behalf Of** Kelvin Liew
Sent: Friday, June 23, 2017 1:38 PM
To: Ballen, Karen <KBallen@liebertpub.com>
Subject: re: thesis reuse of article

[Quoted text hidden]

For Murphy et al. Figure 13, Figure 14, and Figure 15 [20] copyright permissions

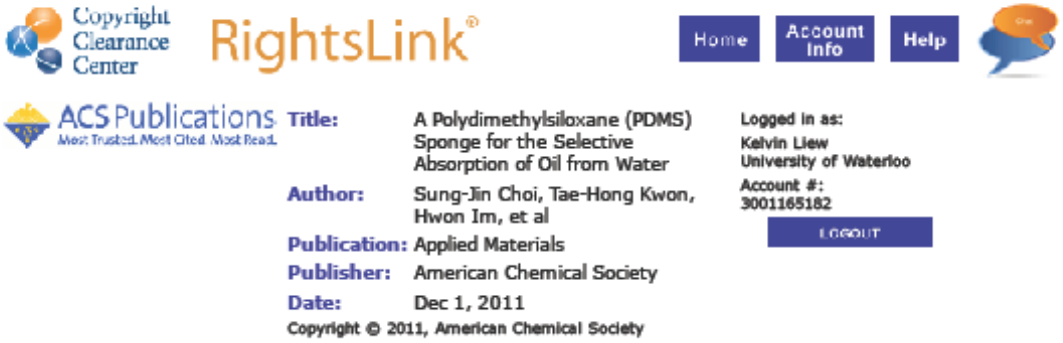

PERMISSION/LICENSE IS GRANTED FOR YOUR ORDER AT NO CHARGE

This type of permission/license, instead of the standard Terms & Conditions, is sent to you because no fee is being charged for your order. Please note the following:

- Permission is granted for your request in both print and electronic formats, and translations.
- If figures and/or tables were requested, they may be adapted or used in part.
- Please print this page for your records and send a copy of it to your publisher/graduate school.
- Appropriate credit for the requested material should be given as follows: "Reprinted (adapted) with permission from (COMPLETE REFERENCE CITATION). Copyright (YEAR) American Chemical Society." Insert appropriate information in place of the capitalized words.
- One-time permission is granted only for the use specified in your request. No additional uses are granted (such as derivative works or other editions). For any other uses, please submit a new request.

If credit is given to another source for the material you requested, permission must be obtained from that source.

BACK CLOSE WINDOW

For Choi et al. Figure 16 and Figure 17 [21] copyright permissions

ROYAL SOCIETY OF CHEMISTRY LICENSE TERMS AND CONDITIONS

Jun 26, 2017

This Agreement between University of Waterloo -- Kelvin Liew ("You") and Royal Society of Chemistry ("Royal Society of Chemistry") consists of your license details and the terms and conditions provided by Royal Society of Chemistry and Copyright Clearance Center.

License Number	4136650218294
License date	Jun 26, 2017
Licensed Content Publisher	Royal Society of Chemistry
Licensed Content Publication	Journal of Materials Chemistry A
Licensed Content Title	Durable superhydrophobic/superoleophilic PDMS sponges and their applications in selective oil absorption and in plugging oil leakages
Licensed Content Author	Xia Zhao,Lingxiao Li,Bucheng Li,Junping Zhang,Aiqin Wang
Licensed Content Date	Sep 12, 2014
Licensed Content Volume	2
Licensed Content Issue	43
Type of Use	Thesis/Dissertation
Requestor type	academic/educational
Portion	figures/tables/images
Number of figures/tables/images	3
Format	print and electronic
Distribution quantity	10
Will you be translating?	no
Order reference number	
Title of the thesis/dissertation	Improving the adhesive properties and fabrication of multilayer biomimetic dry adhesives through the introduction and control of a foam based backing material achieved through sugar cube template moulding technique
Expected completion date	Jul 2017
Estimated size	100
Requestor Location	University of Waterloo 200 University Ave W Waterloo, ON N2L3G1 Canada Attn: University of Waterloo
Billing Type	Invoice
Billing Address	University of Waterloo 200 University Ave W Waterloo, ON N2L3G1

For Zhao et al. Figure 18 and Figure 19 [22] copyright permissions

ROYAL SOCIETY OF CHEMISTRY LICENSE TERMS AND CONDITIONS

Jun 26, 2017

This Agreement between University of Waterloo -- Kelvin Liew ("You") and Royal Society of Chemistry ("Royal Society of Chemistry") consists of your license details and the terms and conditions provided by Royal Society of Chemistry and Copyright Clearance Center.

License Number	4136680456872
License date	Jun 26, 2017
Licensed Content Publisher	Royal Society of Chemistry
Licensed Content Publication	Environmental Science: Water Research & Technology
Licensed Content Title	Selective adsorption of oil–water mixtures using polydimethylsiloxane (PDMS)–graphene sponges
Licensed Content Author	Diana N. H. Tran,Shervin Kabiri,Ting Rui Sim,Dusan Losic
Licensed Content Date	Mar 12, 2015
Licensed Content Volume	1
Licensed Content Issue	3
Type of Use	Thesis/Dissertation
Requestor type	academic/educational
Portion	figures/tables/images
Number of figures/tables/images	3
Format	print and electronic
Distribution quantity	10
Will you be translating?	no
Order reference number	
Title of the thesis/dissertation	Improving the adhesive properties and fabrication of multilayer biomimetic dry adhesives through the introduction and control of a foam based backing material achieved through sugar cube template moulding technique
Expected completion date	Jul 2017
Estimated size	100
Requestor Location	University of Waterloo 200 University Ave W Waterloo, ON N2L3G1 Canada Attn: University of Waterloo
Billing Type	Invoice
Billing Address	University of Waterloo 200 University Ave W Waterloo, ON N2L3G1

For Tran et al. Figure 20 and Figure 21 [23] copyright permissions

ELSEVIER LICENSE
TERMS AND CONDITIONS

Jun 21, 2017

This Agreement between University of Waterloo -- Kelvin Liew ("You") and Elsevier ("Elsevier") consists of your license details and the terms and conditions provided by Elsevier and Copyright Clearance Center.

License Number	4133680504630
License date	Jun 21, 2017
Licensed Content Publisher	Elsevier
Licensed Content Publication	International Journal of Adhesion and Adhesives
Licensed Content Title	Functionally graded dry adhesives based on film-terminated silicone foam
Licensed Content Author	Kelvin Liew,Hamed Shahsavan,Boxin Zhao
Licensed Content Date	Jul 1, 2017
Licensed Content Volume	76
Licensed Content Issue	n/a
Licensed Content Pages	7
Start Page	47
End Page	53
Type of Use	reuse in a thesis/dissertation
Portion	full article
Format	both print and electronic
Are you the author of this Elsevier article?	Yes
Will you be translating?	No
Order reference number	
Title of your thesis/dissertation	Improving the adhesive properties and fabrication of multilayer biomimetic dry adhesives through the introduction and control of a foam based backing material achieved through sugar cube template moulding technique
Expected completion date	Jul 2017
Estimated size (number of pages)	100
Elsevier VAT number	GB 494 6272 12
Requestor Location	University of Waterloo 200 University Ave W Waterloo, ON N2L3G1 Canada Attn: University of Waterloo
Total	0.00 CAD
Terms and Conditions	

For Liew et al. full article [51] copyright permissions

References

[1] R. J. Full, K. Autumn, Y. A. Liang, S. T. Hsieh, W. Zesch, W. P. Chan, T. W. Kenny, and R. Fearing, "Adhesive force of a single gecko foot-hair," *Nature*, vol. 405, no. 6787, pp. 681–685, Jun. 2000.

[2] K. Autumn, P. H. Niewiarowski, and J. B. Puthoff, "Gecko Adhesion as a Model System for Integrative Biology, Interdisciplinary Science, and Bioinspired Engineering," *Annu. Rev. Ecol. Evol. Syst.*, vol. 45, no. 1, pp. 445–470, Nov. 2014.

[3] K. Autumn, M. Sitti, Y. A. Liang, A. M. Peattie, W. R. Hansen, S. Sponberg, T. W. Kenny, R. Fearing, J. N. Israelachvili, and R. J. Full, "Evidence for van der Waals adhesion in gecko setae," *Proc. Natl. Acad. Sci.*, vol. 99, no. 19, pp. 12252–12256, Sep. 2002.

[4] D. Sameoto and C. Menon, "Recent advances in the fabrication and adhesion testing of biomimetic dry adhesives," *Smart Mater. Struct.*, vol. 19, no. 10, p. 103001, Oct. 2010.

[5] H. Shahsavan and B. Zhao, "Bioinspired Functionally Graded Adhesive Materials: Synergetic Interplay of Top Viscous–Elastic Layers with Base Micropillars," *Macromolecules*, vol. 47, no. 1, pp. 353–364, Jan. 2014.

[6] D. Chandra and S. Yang, "Stability of High-Aspect-Ratio Micropillar Arrays against Adhesive and Capillary Forces," *Acc. Chem. Res.*, vol. 43, no. 8, pp. 1080–1091, Aug. 2010.

[7] H. Shahsavan and B. Zhao, "Biologically inspired enhancement of pressure-sensitive adhesives using a thin film-terminated fibrillar interface," *Soft Matter*, vol. 8, no. 32, p. 8281, 2012.

[8] D. Sameoto and C. Menon, "A low-cost, high-yield fabrication method for producing optimized biomimetic dry adhesives," *J. Micromechanics Microengineering*, vol. 19, no. 11, p. 115002, Nov. 2009.

[9] M. P. Murphy, B. Aksak, and M. Sitti, "Gecko-Inspired Directional and Controllable Adhesion," *Small*, vol. 5, no. 2, pp. 170–175, Dec. 2008.

[10] M. P. Murphy, S. Kim, and M. Sitti, "Enhanced Adhesion by Gecko-Inspired Hierarchical Fibrillar Adhesives," *ACS Appl. Mater. Interfaces*, vol. 1, no. 4, pp. 849–855, Apr. 2009.

[11] H. Shahsavan, D. Arunbabu, and B. Zhao, "Biomimetic Modification of Polymeric Surfaces: A Promising Pathway for Tuning of Wetting and Adhesion," *Macromol. Mater. Eng.*, vol. 297, no. 8, pp. 743–760, Aug. 2012.

[12] Thermacore Inc., "Multi-Kilowatt Heat Pipe Heat Sink Performance," *Thermacore Inc.*, 2016. [Online]. Available: http://www.thermacore-europe.com/news/multi-kilowatt-heat-pipe.aspx. [Accessed: 05-Jul-2016].

[13] M. D. Bartlett and A. J. Crosby, "Scaling Normal Adhesion Force Capacity with a Generalized Parameter," *Langmuir*, vol. 29, no. 35, pp. 11022–11027, Sep. 2013.

[14] M. D. Bartlett, A. B. Croll, and A. J. Crosby, "Designing Bio-Inspired Adhesives for Shear Loading: From Simple Structures to Complex Patterns," *Adv. Funct. Mater.*, vol. 22, no. 23, pp. 4985–4992, Dec. 2012.

[15] J. E. Fesmire, B. E. Coffman, B. J. Menghelli, and K. W. Heckle, "Spray-On Foam Insulations for Launch Vehicle Cryogenic Tanks," *Sp. Cryog. Work.*, no. July, 2011.

[16] NASA, "Forty-Year-Old Foam Springs Back With New Benefits," *NASA*, 2005. [Online]. Available: https://spinoff.nasa.gov/Spinoff2005/ch_6.html. [Accessed: 03-Jul-2017].

[17] "Expanded polystyrene packaging," *Expanded Polystyrene Australia Pty Ltd.*, 2014. [Online]. Available: http://epsa.org.au/about-eps/what-is-eps/how-is-eps-made/. [Accessed: 03-Jul-2017].

[18] C. J. Liao, C. F. Chen, J. H. Chen, S. F. Chiang, Y. J. Lin, and K. Y. Chang, "Fabrication of porous biodegradable polymer scaffolds using a solvent merging/particulate leaching method," *J. Biomed. Mater. Res.*, vol. 59, no. 4, pp. 676–681, 2002.

[19] A. Scott, R. Gupta, and G. U. Kulkarni, "A simple water-based synthesis of Au nanoparticle/PDMS composites for water purification and targeted drug release," *Macromol. Chem. Phys.*, vol. 211, no. 15, pp. 1640–1647, 2010.

[20] W. L. Murphy, R. G. Dennis, J. L. Kileny, and D. J. Mooney, "Salt fusion: an approach to improve pore interconnectivity within tissue engineering scaffolds.," *Tissue Eng.*, vol. 8, no. 1, pp. 43–52, 2002.

[21] S.-J. Choi, T.-H. Kwon, H. Im, D.-I. Moon, D. J. Baek, M.-L. Seol, J. P. Duarte, and Y.-K. Choi, "A Polydimethylsiloxane (PDMS) Sponge for the Selective Absorption of Oil from Water," *ACS Appl. Mater. Interfaces*, vol. 3, no. 12, pp. 4552–4556, Dec. 2011.

[22] X. Zhao, L. Li, B. Li, J. Zhang, and A. Wang, "Durable superhydrophobic/superoleophilic PDMS sponges and their applications in selective oil absorption and in plugging oil leakages," *J. Mater. Chem. A*, vol. 2, no. 43, pp. 18281–18287, 2014.

[23] D. N. H. Tran, S. Kabiri, T. R. Sim, and D. Losic, "Selective adsorption of oil–water mixtures using polydimethylsiloxane (PDMS)–graphene sponges," *Environ. Sci. Water Res. Technol*, vol. 1, no. 1, pp. 298–305, 2014.

[24] N. Nadermann, J. Ning, A. Jagota, and C.-Y. Hui, "Active Switching of Adhesion in a Film-Terminated Fibrillar Structure," *Langmuir*, vol. 26, no. 19, pp. 15464–15471, Oct. 2010.

[25] A. Miserez, T. Schneberk, C. Sun, F. W. Zok, and J. H. Waite, "The Transition from Stiff to Compliant Materials in Squid Beaks," *Science (80-.).*, vol. 319, no. 5871, pp. 1816–1819, Mar. 2008.

[26] S. M. Kang, "Bioinspired design and fabrication of green-environmental dry adhesive with robust wide-tip shape," *Int. J. Precis. Eng. Manuf. Technol.*, vol. 3, no. 2, pp. 189–192, Apr. 2016.

[27] E. W. Hawkes, D. L. Christensen, Amy Kyungwon Han, H. Jiang, and M. R. Cutkosky, "Grasping without squeezing: Shear adhesion gripper with fibrillar thin film," in *2015 IEEE International Conference on Robotics and Automation (ICRA)*, 2015, vol. 2, no. 1, pp. 2305–2312.

[28] H. Shahsavan, S. M. Salili, A. Jákli, and B. Zhao, "Smart Muscle-Driven Self-Cleaning of Biomimetic Microstructures from Liquid Crystal Elastomers," *Adv. Mater.*, vol. 27, no. 43, pp. 6828–6833, Nov. 2015.

[29] A. del Campo, C. Greiner, I. Álvarez, and E. Arzt, "Patterned Surfaces with Pillars with Controlled 3D Tip Geometry Mimicking Bioattachment Devices," *Adv. Mater.*, vol. 19, no. 15, pp. 1973–1977, Aug. 2007.

[30] H. E. Jeong, J.-K. Lee, H. N. Kim, S. H. Moon, and K. Y. Suh, "A nontransferring dry adhesive with hierarchical polymer nanohairs," *Proc. Natl. Acad. Sci.*, vol. 106, no. 14, pp. 5639–5644, Apr. 2009.

[31] H. Shahsavan and B. Zhao, "Conformal Adhesion Enhancement on Biomimetic Microstructured Surfaces," *Langmuir*, vol. 27, no. 12, pp. 7732–7742, Jun. 2011.

[32] A. Majumder, A. Ghatak, and A. Sharma, "Microfluidic Adhesion Induced by Subsurface Microstructures," *Science (80-.).*, vol. 318, no. 5848, pp. 258–261, Oct. 2007.

[33] W.-G. Bae, D. Kim, and K.-Y. Suh, "Instantly switchable adhesion of bridged fibrillar adhesive via gecko-inspired detachment mechanism and its application to a transportation system," *Nanoscale*, vol. 5, no. 23, p. 11876, 2013.

[34] M. Zhou, N. Pesika, H. Zeng, Y. Tian, and J. Israelachvili, "Recent advances in gecko adhesion and friction mechanisms and development of gecko-inspired dry adhesive surfaces," *Friction*, vol. 1, no. 2, pp. 114–129, Jun. 2013.

[35] A. Jagota and C.-Y. Hui, "Adhesion, friction, and compliance of bio-mimetic and bio-inspired structured interfaces," *Mater. Sci. Eng. R Reports*, Oct. 2011.

[36] S. Kim, M. Sitti, C.-Y. Hui, R. Long, and A. Jagota, "Effect of backing layer thickness on adhesion of single-level elastomer fiber arrays," *Appl. Phys. Lett.*, vol. 91, no. 16, p. 161905, Oct. 2007.

[37] N. Gupta, "A functionally graded syntactic foam material for high energy absorption under compression," *Mater. Lett.*, vol. 61, no. 4–5, pp. 979–982, Feb. 2007.

[38] L. J. Gibson and M. F. Ashby, *Cellular solids: Structure and properties*, vol. 123. 1990.

[39] D. H. Kim, M. C. Jung, S.-H. Cho, S. H. Kim, H.-Y. Kim, H. J. Lee, K. H. Oh, and M.-W. Moon, "UV-responsive nano-sponge for oil absorption and desorption," *Sci. Rep.*, vol. 5, p. 12908, Aug. 2015.

[40] A. Turco, C. Malitesta, G. Barillaro, A. Greco, A. Maffezzoli, and E. Mazzotta, "A magnetic and highly reusable macroporous superhydrophobic/superoleophilic PDMS/MWNT nanocomposite for oil sorption from water," *J. Mater. Chem. A*, vol. 3, no. 34, pp. 17685–17696, 2015.

[41] N. J. Glassmaker, A. Jagota, C.-Y. Hui, W. L. Noderer, and M. K. Chaudhury, "Biologically inspired crack trapping for enhanced adhesion," *Proc. Natl. Acad. Sci.*, vol. 104, no. 26, pp. 10786–10791, Jun. 2007.

[42] K. R. Shull, "Contact mechanics and the adhesion of soft solids," *Mater. Sci. Eng. R Reports*, vol. 36, no. 1, pp. 1–45, Jan. 2002.

[43] T. Thomas and A. J. Crosby, "Controlling Adhesion with Surface Hole Patterns," *J. Adhes.*, vol. 82, no. 3, pp. 311–329, Apr. 2006.

[44] H. X. Zhu and A. H. Windle, "Effects of cell irregularity on the high strain compression of open-cell foams," *Acta Mater.*, vol. 50, no. 5, pp. 1041–1052, Mar. 2002.

[45] M. W. Schraad and F. H. Harlow, "A stochastic constitutive model for disordered cellular materials: Finite-strain uni-axial compression," *Int. J. Solids Struct.*, vol. 43, no. 11–12, pp. 3542–3568, Jun. 2006.

[46] W. L. Noderer, L. Shen, S. Vajpayee, N. J. Glassmaker, A. Jagota, and C.-Y. Hui, "Enhanced adhesion and compliance of film-terminated fibrillar surfaces," *Proc. R. Soc. A Math. Phys. Eng. Sci.*, vol. 463, no. 2086, pp. 2631–2654, Oct. 2007.

[47] C. Menon, M. Murphy, and M. Sitti, "Gecko Inspired Surface Climbing Robots," in *2004 IEEE International Conference on Robotics and Biomimetics*, 2004, pp. 431–436.

[48] S. Song and M. Sitti, "Soft Grippers Using Micro-fibrillar Adhesives for Transfer Printing," *Adv. Mater.*, vol. 26, no. 28, pp. 4901–4906, Jul. 2014.

[49] Y. Mengüç, S. Y. Yang, S. Kim, J. A. Rogers, and M. Sitti, "Gecko-Inspired Controllable Adhesive Structures Applied to Micromanipulation," *Adv. Funct. Mater.*, vol. 22, no. 6, pp. 1246–1254, Mar. 2012.

[50] J. Purtov, M. Frensemeier, and E. Kroner, "Switchable Adhesion in Vacuum Using Bio-Inspired Dry Adhesives," *ACS Appl. Mater. Interfaces*, vol. 7, no. 43, pp. 24127–24135, Nov. 2015.

[51] K. Liew, H. Shahsavan, and B. Zhao, "Functionally graded dry adhesives based on f ilm-terminated silicone foam," *Int. J. Adhes. Adhes.*, vol. 76, no. xxxx, pp. 47–53, Jul. 2017.

[52] D. Sameoto and C. Menon, "Deep UV patterning of acrylic masters for molding biomimetic dry adhesives," *J. Micromechanics Microengineering*, vol. 20, no. 11, p. 115037, Nov. 2010.

[53] P. Y. Isla and E. Kroner, “A Novel Bioinspired Switchable Adhesive with Three Distinct Adhesive States,” *Adv. Funct. Mater.*, vol. 25, no. 16, pp. 2444–2450, Apr. 2015.

Appendices

Table 7: Preload pull-off force values

Sample	Tests	Preload $[N]$	STDEV	Pull-off $[N]$	STDEV
C	2	0.11	0.01	0.44	0.12
	2	0.21	0.01	0.47	0.06
	3	0.32	0.02	0.42	0.13
	3	0.41	0.01	0.43	0.12
	4	0.52	0.03	0.42	0.11
	5	1.06	0.19	0.47	0.00
	5	1.98	0.08	0.49	0.12
	4	2.98	0.04	0.49	0.13
	4	4.03	0.06	0.50	0.13
	4	5.03	0.06	0.50	0.13
Film foam	5	0.10	0.01	0.17	0.08
	5	0.19	0.01	0.20	0.07
	5	0.29	0.02	0.21	0.06
	5	0.39	0.02	0.23	0.04
	5	0.49	0.02	0.24	0.04
	5	0.98	0.03	0.26	0.04
	5	1.97	0.06	0.29	0.05
	5	2.96	0.08	0.30	0.06
	5	3.94	0.12	0.30	0.06
	4	5.00	0.00	0.32	0.05
Micro block	2	0.11	0.01	0.55	0.07
	2	0.21	0.02	0.74	0.05
	2	0.31	0.01	0.85	0.04
	3	0.42	0.02	1.00	0.13
	3	0.52	0.02	1.04	0.10
	4	1.02	0.02	1.20	0.08
	4	2.02	0.03	1.28	0.07
	4	3.00	0.03	1.25	0.05
	4	4.01	0.02	1.23	0.05
	4	4.95	0.06	1.17	0.09
Micro foam	5	0.10	0.01	0.55	0.13
	5	0.20	0.01	0.74	0.12
	5	0.29	0.01	0.88	0.12
	5	0.39	0.01	0.97	0.08
	5	0.49	0.02	1.06	0.06
	5	0.99	0.03	1.29	0.11
	5	1.98	0.05	1.55	0.12
	5	2.97	0.07	1.75	0.23
	5	3.95	0.10	1.80	0.26
	4	5.00	0.00	1.79	0.27
Macro block	2	0.10	0.01	0.22	0.04
	2	0.20	0.01	0.27	0.01
	2	0.31	0.02	0.30	0.01
	2	0.41	0.02	0.35	0.03
	3	0.51	0.01	0.39	0.04

Sample	Tests	Preload [N]	STDEV	Pull-off [N]	STDEV
Macro block *(cont'd)*	3	0.99	0.03	0.47	0.05
	4	1.90	0.17	0.52	0.02
	5	2.88	0.28	0.56	0.04
	5	3.99	0.04	0.57	0.03
	4	4.96	0.06	0.56	0.03
Macro foam	5	0.10	0.01	0.29	0.11
	5	0.19	0.01	0.45	0.16
	5	0.29	0.02	0.55	0.17
	5	0.39	0.02	0.70	0.18
	5	0.49	0.02	0.82	0.24
	5	0.98	0.03	1.06	0.19
	5	1.97	0.06	1.28	0.12
	5	2.96	0.08	1.33	0.12
	5	3.95	0.11	1.34	0.11
	4	5.00	0.00	1.32	0.12